Optimal Detection Interval for Absorbing Receivers in Molecular Communication Systems With Interference

Trang Ngoc Cao, *Member, IEEE*, Nikola Zlatanov, *Member, IEEE*, Phee Lep Yeoh, *Member, IEEE*, and Jamie S. Evans, *Senior Member, IEEE*

***Abstract*—We consider a molecular communication system comprised of a transmitter, an absorbing receiver, and an interference source. Assuming amplitude modulation, we analyze the dependence of the bit error rate (BER) on the detection interval, which is the time within one transmission symbol interval during which the receiver is active to absorb and detect the number of information-carrying molecules. We then propose efficient algorithms to determine the optimal detection interval that minimizes the BER of the molecular communication system assuming no inter-symbol interference (ISI). Simulation and numerical evaluations are provided to highlight further insights into the optimal results. For example, we demonstrate that the optimal detection interval can be very small compared to the transmission symbol interval. Moreover, our numerical results show that significant BER improvements are achieved by using the optimal detection interval for systems without and with ISI.**

***Index Terms*—Molecular communications, interference, optimization, detection, absorbing receiver.**

I. Introduction

Molecular communications (MC) is an exciting new paradigm that overcomes fundamental limits of size and operating environments in traditional radio frequency (RF)-based communication systems. Molecular communications is well-suited to challenging environments such as tunnels, pipelines, or salt water, where RF waves suffer extreme attenuation [2]. In addition, molecular communications is biocompatible and therefore can be used in human bodies for health monitoring, disease detection, or drug delivery [3].

A promising platform for molecular communications is nano-machines, which will be able to perform more complex tasks if they can mutually communicate. Since each nano-machine can perform simple operations, an essential requirement in molecular communications is simplicity. For example, simple modulation techniques are typically used in molecular communications, such as amplitude modulation, where information is embedded into the number of released molecules at the transmitter. In addition, the molecular receivers operating these modulation techniques should have a simple structure. Two general types of molecular receivers for amplitude modulation have been proposed in the literature so far; a passive and an absorbing receiver. A passive receiver is a receiver that observes and counts molecules in the receiving area at a specific sampling instant without disrupting the movement of the molecules. An absorbing receiver is a receiver that absorbs and counts molecules reaching the receiver within a given detection interval. Both passive and absorbing receivers can be realized by artificial cells or nano-machines [4], [5]. We note that more advanced variations of these two simple receiver models such as the temporarily binding receiver [6] and reactive receiver [7] have also been proposed in the literature.

In general, the performance of a molecular communication system can be improved by adjusting the sampling instants for passive receivers or the detection interval for absorbing receivers. This article investigates the latter and proposes algorithms that optimize the detection interval of an absorbing receiver in order to minimize the bit error rate (BER) when the molecular communication system is affected by an unintended transmitter from another communication link. This is motivated by the fact that if a molecular communication system for nano-machines would be deployed in a real environment, the communication session would experience interference from various external sources such as biochemical processes, leaking vesicles, or other unintended transmitters [8]. In particular, sensor networks may have multiple communication links using the same type of molecules and the same designs of transmitters and receivers since the options of suitable molecular types and their corresponding transceivers' designs, e.g., suitable sensors, in a specific environment can be limited and a unified design is convenient to expand the network. Hence, transmitters from these communication links result in external interference to each other, which has not been considered in the literature. Since nano-machine require simplicity, we need to find a simple solution to mitigate the impact of the

Manuscript received April 30, 2020; revised August 4, 2020; accepted September 15, 2020. Date of publication September 29, 2020; date of current version November 13, 2020. This work was supported in part by the Australian Research Council Discovery Projects under Grant DP180101205. This paper was presented in part at the IEEE International Conference on Communications 2018 [1]. *(Corresponding author: Trang Ngoc Cao.)*

Trang Ngoc Cao and Jamie S. Evans are with the Department of Electrical and Electronic Engineering, University of Melbourne, Melbourne, VIC 3010, Australia (e-mail: ngocc@student.unimelb.edu.au; jse@unimelb.edu.au).

Nikola Zlatanov is with the Department of Electrical and Computer Systems Engineering, Monash University, Melbourne, VIC 3800, Australia (e-mail: nikola.zlatanov@monash.edu).

Phee Lep Yeoh is with the School of Electrical and Information Engineering, University of Sydney, Sydney, NSW 2006, Australia (e-mail: phee.yeoh@sydney.edu.au).

Digital Object Identifier 10.1109/TMBMC.2020.3027250

interference. Related works on BER in molecular communication systems with multiple transmitters include papers such as [8] and [9]. However, in these works, the detection interval is equal to the transmission symbol interval.

For passive receivers, the optimal sampling instant at which the receiver observes the largest number of molecules within one transmission symbol interval was derived in [10] and [11]. In [12], a passive receiver that observes multiple sampling instants during each transmission symbol interval was considered and maximum-likelihood detection was applied across all observation samples. Thereby, it was observed that the BER decreases when the number of samples increases, which is intuitive since more information is received. Recently, approximate closed-form expressions for the optimal number of samples and the optimal position of each sample within one transmission symbol interval that minimize the BER were analyzed in [13].

For absorbing receivers, most existing works [14]–[16] assume that the detection interval is equal to the transmission symbol interval. Exceptions are the works in [13], [17]–[19], which considered variable detection intervals. However, [13], [17]–[19] did not consider the impact of external interference from an unintended transmitter when optimizing the detection interval in terms of the system performance and only considered the internally generated inter-symbol interference (ISI) and constant-mean noise from the environment. The detection interval was optimized for minimizing the BER in [13], [17], [19], and for maximizing the capacity in [18].[1] Moreover, [13], [17], [18] determined the optimal detection time interval by exhaustive search, whereas [19] derives an approximately optimal detection time interval. Whereas, in this work, we consider both ISI and external interference from an unintended transmitter, whose *conditional mean in each symbol interval varies* depending if the unintended transmitter transmits bits "0" or "1". Thereby, we propose two efficient algorithms to optimize the detection interval for minimizing the BER in a one dimensional (1D) MC system, which finds application in long narrow tube environments, and a three dimensional (3D) MC system, which finds application in free-space environments. We consider the most simple case, i.e., the 1D system, and the most general case, i.e., the 3D system, as the two dimensional system can be straightforwardly analyzed by using the same framework.

In this article, we use the Binomial distribution to accurately describe the number of received molecules at the absorbing receiver [20], [21]. In addition, the Poisson and Gaussian distributions are also used since they provide an approximation of the number of received molecules which is much easier to analyze [8], [9], [11]–[13], [15], [16], [22], [23]. However, note that the accuracy of the Poisson and Gaussian distributions does not always hold, as discussed in [20] and [24]. We investigate the molecular communication system both in a 1D space as in [25] and [26] as well as in a 3D space as in [11]–[13]. In addition, we investigate the interesting case, from a practical perspective, of an interference source with an unknown location in a 1D system, which has not been considered in the literature so far. Our numerical results show that using the optimal detection interval, obtained by our proposed algorithms, leads to high performance in terms of BER.

The main contributions of this work can be summarized as follows:

- We derive the BER of a MC system affected by external interference from another communication link in 1D and 3D environments, when the system is impaired and is not impaired by ISI and when maximum likelihood (ML) detection is used. We consider three cases, i.e., when the Binomial, Poisson, and Gaussian distributions are used for the analysis, respectively.
- We optimize the detection interval and show that the system performance in terms of BER is improved significantly by choosing a suitable detection interval, for which we design a simple algorithm.
- We optimize the detection interval and improve the BER even when the interference is at an unknown location in a 1D system.

This paper expands its conference version [1] where the analysis with approximations, i.e., when the Poisson and Gaussian distributions are used, and the ISI impact on the system are not included.

The remainder of this article is organized as follows. In Section II, we introduce the system and channel models for 1D and 3D environments. In Section III, we construct an optimization problem of the optimal detection interval and derive the BER of the systems. Section IV proposes algorithms that optimize the detection interval in terms of BER. Section V extends the investigation of the optimal detection interval to an interference source at an unknown location. Numerical results are provided in Section VI, and Section VII concludes this article.

II. System and Channel Models

In the following, we present the system and channel models for our proposed molecular communication systems with interference.

A. System Model

We consider a 1D unbounded MC system and a 3D unbounded MC system. The 1D system is comprised of a point transmitter Tx, a point absorbing receiver Rx, and a point interference source Ix. The interference source Ix is assumed to be a transmitter from another communication link that employs the same modulation and molecule type as Tx. Rx is assumed to be at distances d and d_{I} from Tx and Ix, respectively, as shown in Fig. 1. The 3D system is comprised of a spherical absorbing receiver Rx with radius a_{rx}, a point transmitter Tx at a distance d from the center of the receiver, and a point interference source Ix at a distance d_{I} from the center of the receiver, as shown in Fig. 2. Note that the Tx and Ix do not need to be located on one side of the Rx in a 1D system or be aligned with Rx in a 3D system. The analysis in this article applies to any relative positions of the transceivers that satisfies their respective distances. We assume that the movement of the molecules in space follows a Brownian motion [27]. We assume that both the intended and interfering transmitters, Tx

[1]The period length τ in which molecules are absorbed by the receivers and removed from the environment, i.e., the period that is not the detection interval, was investigated and defined in [17] as the cleanse time.

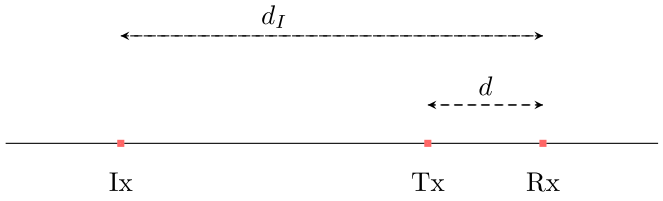

Fig. 1. 1D system model comprised of a transmitter, Tx, an interference source, Ix, and a receiver, Rx.

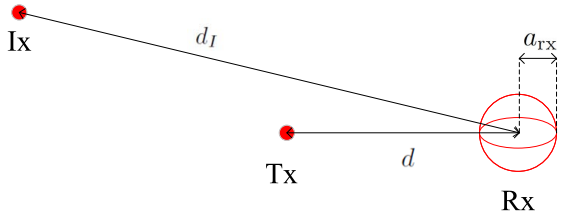

Fig. 2. 3D system model comprised of a transmitter, Tx, an interference source, Ix, and a receiver, Rx.

and Ix, do not affect the diffusion of the molecules after they are released at the transmitters and that the receiver absorbs all molecules that reach it.

We assume amplitude modulation, i.e., that information bits are modulated by the number of released molecules from the transmitter. Let the number of released molecules at Tx during the j-th transmission symbol interval be denoted by $X_{\mathrm{T}}^{(j)}$, where $X_{\mathrm{T}}^{(j)} \in \{N_0, N_1\}$, $N_1 > N_0$. For brevity, we use X_{T} for arbitrary j, i.e., when there is no need to specify j. When $X_{\mathrm{T}} = N_0$, then bit "0" is assumed to be transmitted and when $X_{\mathrm{T}} = N_1$, then bit "1" is assumed to be transmitted. We consider $X_{\mathrm{T}} \in \{N_0, N_1\}$ instead of on-off keying to generalize the analysis so that it can be applied to higher-order modulation, e.g., $X_{\mathrm{T}} \in \{N_0, N_1, N_2, N_3\}$, in future work. This is also motivated by the fact that using a zero release rate of molecules is not common in cell signaling in nature [28]. We assume that the bits transmitted by Tx are uncoded. As a result, the receiver is assumed to perform bit-by-bit detection of the received molecules. For the interference transmitter, the number of molecules released by Ix during the transmission symbol interval j is denoted by $X_{\mathrm{I}}^{(j)}$, where $X_{\mathrm{I}}^{(j)} \in \{N_0, N_1\}$. Similar to $X_{\mathrm{T}}^{(j)}$, for brevity, we use X_{I} for arbitrary j, i.e., when there is no need to specify j. We assume that the transmitted bits from Tx and Ix have equal-probabilities of occurrence defined, respectively, as

$$P_{X_{\mathrm{T}}}(x_{\mathrm{T}} = N_0) = P_{X_{\mathrm{T}}}(x_{\mathrm{T}} = N_1) = \frac{1}{2} \tag{1}$$

and

$$P_{X_{\mathrm{I}}}(x_{\mathrm{I}} = N_0) = P_{X_{\mathrm{I}}}(x_{\mathrm{I}} = N_1) = \frac{1}{2}. \tag{2}$$

Let T_{b} denote the duration of the transmission symbol interval during which one information bit is transmitted at Tx. We assume instantaneous release and molecules are released at the beginning of T_{b}. Let T_{r} denote the duration of the detection symbol interval during which Rx absorbs and counts the number of absorbed molecules in order to detect a transmitted information bit. We assume that Tx, Ix, and Rx are synchronized, which can be done using already available techniques in the literature such as the peak of the received molecular signal [29], [30], the arrival time of the molecules [31], the probability of molecules hitting a receiver [32], a two-way message exchange between the two nanomachines [33], two types of molecules for synchronization and data transmission [34], [35]. For synchronization with living entities or biochemical processes, other techniques such as exchanging molecules between bacteria and cells, electrical stimulation, and mechanical stimulation may also be applied, see [36]–[41] and references therein. To focus on the proposed design, synchronization between the transceivers, i.e., the receiver starts receiving molecules when the transmitter releases molecules, is a fair assumption which has been made in the literature [42]–[45]. We note that synchronization is crucial for the system especially in 3D scenarios and large distances where the BER is high. As such, designing simple and practical synchronization approaches for MC is an important topic to be considered in future works. Here, we assume that the transmission symbol intervals of Tx and Ix have the same duration and start at the same instant, which is also the starting instant of T_{r}.

Remark 1: For a simple receiver without memory, the detection symbol intervals cannot overlap with each other, i.e., each detection symbol interval must start after the previous one has ended. In addition, T_{r} must be less or equal to T_{b}, i.e., $T_{\mathrm{r}} \leq T_{\mathrm{b}}$ has to hold. Otherwise, if $T_{\mathrm{r}} > T_{\mathrm{b}}$, the detection symbol interval for the j-th transmitted bit ($j \gg 1$) will start after a long period from the start of the j-th bit transmission symbol interval. In that case, the probability of receiving molecules belonging to the j-th bit approaches zero as j increases, since most of those molecules would be absorbed in the previous detection symbol intervals. Note that, at time t, where $T_{\mathrm{r}} < t < T_{\mathrm{b}}$, molecules should still be absorbed at Rx in order to limit ISI. However, we assume that these molecules are not included in the decision of the considered bit.

B. Channel Model

At the receiver, the information bits are detected based on the number of absorbed molecules during the detection symbol interval T_{r}. Let $Y_{\mathrm{T}}^{(j)}$ and $Y_{\mathrm{I}}^{(j)}$ denote the number of received molecules at Rx during the interval T_{r} of the j-th bit which are released from Tx and Ix at the beginning of the j-th bit interval, respectively. Then, according to [20], $Y_{\mathrm{T}}^{(j)}$ and $Y_{\mathrm{I}}^{(j)}$ follow Binomial distributions, i.e., $Y_{\mathrm{T}}^{(j)} \sim \mathsf{Binom}(X_{\mathrm{T}}^{(j)}, p_d)$ and $Y_{\mathrm{I}}^{(j)} \sim \mathsf{Binom}(X_{\mathrm{I}}^{(j)}, p_{d_{\mathrm{I}}})$, respectively, where $X_{\mathrm{T}}^{(j)}$, p_d, $X_{\mathrm{I}}^{(j)}$, and $p_{d_{\mathrm{I}}}$ are parameters of the distributions. In particular, p_d and $p_{d_{\mathrm{I}}}$ are the probabilities that a molecule released from Tx and Ix at the beginning of T_{b} arrives at Rx, placed at distance d from Tx and d_{I} from Ix, within the interval T_{r}, respectively. Similar to X_{T} and X_{I}, for brevity, we use Y_{T} and Y_{I} for arbitrary j, i.e., when there is no need to specify j.

The probability mass function (PMF) of Y_{T} conditioned on X_{T} is given by

$$P_{Y_{\mathrm{T}}|X_{\mathrm{T}}}(y_{\mathrm{T}}|x_{\mathrm{T}}) = \binom{x_{\mathrm{T}}}{y_{\mathrm{T}}} p_d^{y_{\mathrm{T}}} (1-p_d)^{x_{\mathrm{T}}-y_{\mathrm{T}}}. \tag{3}$$

The PMF of Y_{I} conditioned on X_{I} is then given by

$$P_{Y_{\mathrm{I}}|X_{\mathrm{I}}}(y_{\mathrm{I}}|x_{\mathrm{I}}) = \binom{x_{\mathrm{I}}}{y_{\mathrm{I}}} p_{d_{\mathrm{I}}}^{y_{\mathrm{I}}} (1-p_{d_{\mathrm{I}}})^{x_{\mathrm{I}}-y_{\mathrm{I}}}. \tag{4}$$

In a 1D unbounded environment, p_d and p_{d_I} are given, respectively, by [2]

$$p_d = \mathrm{erfc}\left(\frac{d}{2\sqrt{DT_\mathrm{r}}}\right), \tag{5}$$

$$p_{d_\mathrm{I}} = \mathrm{erfc}\left(\frac{d_\mathrm{I}}{2\sqrt{DT_\mathrm{r}}}\right), \tag{6}$$

where $\mathrm{erfc}(.)$ is the complementary error function and D is the diffusion coefficient.

In a 3D unbounded environment, p_d and p_{d_I} are given respectively by [2], [46]

$$p_d = \frac{r}{d}\mathrm{erfc}\left(\frac{d-r}{2\sqrt{DT_\mathrm{r}}}\right), \tag{7}$$

$$p_{d_\mathrm{I}} = \frac{r}{d_\mathrm{I}}\mathrm{erfc}\left(\frac{d_\mathrm{I}-r}{2\sqrt{DT_\mathrm{r}}}\right). \tag{8}$$

Since we consider Ix from an unintended transmitter, transmitting to a different absorbing receiver, the absorbing receiver of the unintended transmitter can affect the absorptions of the molecules transmitted from Tx. Thus, the number of absorbed molecules at Rx may be reduced compared to the case when there is only one absorbing receiver. A few works have considered this effect [47]–[49]. In [47], the interference receiver is assumed to be located at specific positions, i.e., aligned on a line or on a circle on the same plane with the transmitter and the target receiver. In [48], the impact of the two receivers on each other was investigated by simulation. In [49], a channel model was proposed based on a simulation fitting algorithm. However, in this work, we assume that this effect is negligible. In fact, for the parameters chosen in this work, it is shown in Section VI that the impact is not significant. The results in the literature that investigate this effect can be applied in our proposed framework by using the corresponding expressions of p_d and p_{d_I} impacted by two receivers.

In the following, we first formulate the general problem for optimizing the detection interval, T_r, that minimizes the BER. We then assume the system is without ISI in order to derive the optimal detection and a tractable BER expression that can be used for optimizing T_r. Next, we derive the optimal detection for the system with ISI and discuss the optimization of T_r for this system.

III. Problem Formulation and Detections

A. Problem Formulation

The absorbing receiver detects the transmitted information based on the number of received molecules. Moreover, the numbers of information and interference molecules received at Rx, i.e., Y_T and Y_I, depend on p_d and p_{d_I}, respectively, and thus depend on T_r due to (7) and (8). Therefore, the BER of the system, denoted by P_b, is a function of T_r. Since T_r can be varied at the receiver, we can find the optimal detection interval $T_\mathrm{r}^\star$ that minimizes the BER. More precisely, $T_\mathrm{r}^\star$ is found from the following optimization problem

$$T_\mathrm{r}^\star = \underset{0\le T_\mathrm{r}\le T_\mathrm{b}}{\arg\min}\, P_\mathrm{b}. \tag{9}$$

In order to solve the optimization problem in (9), we need to find the expression of the BER as a function of T_r.

In order to focus on the effect of interference from Ix and find a simple expression of the BER, we first assume that the ISI is negligible at the Rx. This assumption becomes valid by setting the transmission symbol interval T_b to be long enough such that most of the molecules transmitted from previous transmission symbol intervals arrive at the Rx, such as in [26] and [50], or by using enzymes to react with the remaining molecules in the environment, such as in [20].

In order for the detection process to be optimal, in terms of minimizing the BER, we consider ML detection at the receiver. We first consider a ML detection for the system assuming no ISI in order to solve the optimization problem (9). We then consider a ML detection for the systems with ISI.

B. Maximum Likelihood Detection Without ISI

For the ML detection, the receiver decides whether $X_\mathrm{T} = N_0$ or $X_\mathrm{T} = N_1$ based on the following decision function

$$\hat{X}_\mathrm{T} = \underset{X_\mathrm{T}\in\{N_0,N_1\}}{\arg\max}\, P_{Y|X_\mathrm{T}}(y|x_\mathrm{T}), \tag{10}$$

where $\hat{X}_\mathrm{T}$ is the detection of X_T, Y is the total number of molecules received at the receiver during the detection symbol interval T_r from both transmitters, given by

$$Y = Y_\mathrm{T} + Y_\mathrm{I}, \tag{11}$$

and $P_{Y|X_\mathrm{T}}(y|x_\mathrm{T})$ is the conditional PMF of the total number of received molecules, Y, conditioned on the number of transmitted molecules from Tx being X_T. Assuming no ISI, $P_{Y|X_\mathrm{T}}(y|x_\mathrm{T})$ can be obtained as

$$\begin{aligned} P_{Y|X_\mathrm{T}}(y|x_\mathrm{T}) = {} & P_{Y|X_\mathrm{T},X_\mathrm{I}}(y|x_\mathrm{T}, x_\mathrm{I}=N_0)P_{X_\mathrm{I}}(x_\mathrm{I}=N_0) \\ & + P_{Y|X_\mathrm{T},X_\mathrm{I}}(y|x_\mathrm{T}, x_\mathrm{I}=N_1)P_{X_\mathrm{I}}(x_\mathrm{I}=N_1), \end{aligned} \tag{12}$$

where $P_{Y|X_\mathrm{T},X_\mathrm{I}}(y|x_\mathrm{T}, x_\mathrm{I})$ is the conditional probability of receiving Y molecules at the receiver when X_T and X_I molecules are released from the transmitters Tx and Ix, respectively, and $P_{X_\mathrm{I}}(x_\mathrm{I})$ is the probability of releasing X_I molecules from Ix.

Let $\mathbb{Z}_0$ and $\mathbb{Z}_1$ be two sets comprised of numbers of received molecules, Y, for which the probability $P_{Y|X_\mathrm{T}}(y|x_\mathrm{T}=N_0)$ is larger than the probability $P_{Y|X_\mathrm{T}}(y|x_\mathrm{T}=N_1)$ and vice versa, respectively. Then, (10) is equivalent to the following

$$\begin{aligned} \hat{X}_\mathrm{T} &= \underset{X_\mathrm{T}\in\{N_0,N_1\}}{\arg\max}\, P_{Y|X_\mathrm{T}}(y|x_\mathrm{T}) \\ &= \begin{cases} N_0, \text{if} P_{Y|X_\mathrm{T}}(y|x_\mathrm{T}=N_0) > P_{Y|X_\mathrm{T}}(y|x_\mathrm{T}=N_1) \\ N_1, \text{if} P_{Y|X_\mathrm{T}}(y|x_\mathrm{T}=N_1) \ge P_{Y|X_\mathrm{T}}(y|x_\mathrm{T}=N_0) \end{cases} \\ &= \begin{cases} N_0, \text{if} y \in \mathbb{Z}_0 \\ N_1, \text{if} y \in \mathbb{Z}_1. \end{cases} \end{aligned} \tag{13}$$

The sets $\mathbb{Z}_0$ and $\mathbb{Z}_1$ can be obtained by comparing $P_{Y|X_\mathrm{T}}(y|x_\mathrm{T}=N_0)$ and $P_{Y|X_\mathrm{T}}(y|x_\mathrm{T}=N_1)$ for each y in the interval $0 \le y \le 2N_1$. Note that the sets $\mathbb{Z}_0$ and $\mathbb{Z}_1$ can be calculated offline by the system designer and then stored at the receiver. For optimal detection, the receiver only needs to compare whether the received number of molecules, Y, belongs to the set $\mathbb{Z}_0$ or the set $\mathbb{Z}_1$ and make a decision using (13).

Hence, the computational complexity of the proposed decision rule is low, which makes it suitable for a simple receiver.

Having defined the decision rule, given by (13), the BER can be obtained as

$$P_{\mathrm{b}} = P_{\hat{X}_{\mathrm{T}}|X_{\mathrm{T}}}(\hat{x}_{\mathrm{T}} = N_0|x_{\mathrm{T}} = N_1)P_{X_{\mathrm{T}}}(x_{\mathrm{T}} = N_1) + P_{\hat{X}_{\mathrm{T}}|X_{\mathrm{T}}}(\hat{x}_{\mathrm{T}} = N_1|x_{\mathrm{T}} = N_0)P_{X_{\mathrm{T}}}(x_{\mathrm{T}} = N_0), \tag{14}$$

where $P_{\hat{X}_{\mathrm{T}}|X_{\mathrm{T}}}(\hat{x}_{\mathrm{T}}|x_{\mathrm{T}})$ is the PMF of detecting $\hat{X}_{\mathrm{T}}$ given that X_{T} was transmitted at Tx, and $P_{X_{\mathrm{T}}}(x_{\mathrm{T}})$ is the probability of releasing X_{T} molecules at Tx.

Now, to derive the BER as a function of T_{r} from (14), we first need to find $P_{\hat{X}_{\mathrm{T}}|X_{\mathrm{T}}}(\hat{x}_{\mathrm{T}}|x_{\mathrm{T}})$. To this end, we use (13). Due to (13), we have

$$P_{\hat{X}_{\mathrm{T}}}(\hat{x}_{\mathrm{T}} = N_0) = \sum_{y\in\mathbb{Z}_0} P_Y(y), \tag{15}$$

and

$$P_{\hat{X}_{\mathrm{T}}}(\hat{x}_{\mathrm{T}} = N_1) = \sum_{y\in\mathbb{Z}_1} P_Y(y). \tag{16}$$

Thereby,

$$P_{\hat{X}_{\mathrm{T}}|X_{\mathrm{T}}}(\hat{x}_{\mathrm{T}} = N_0|x_{\mathrm{T}} = N_1) = \sum_{y\in\mathbb{Z}_0} P_{Y|X_{\mathrm{T}}}(y|x_{\mathrm{T}} = N_1), \tag{17}$$

and

$$P_{\hat{X}_{\mathrm{T}}|X_{\mathrm{T}}}(\hat{x}_{\mathrm{T}} = N_1|x_{\mathrm{T}} = N_0) = \sum_{y\in\mathbb{Z}_1} P_{Y|X_{\mathrm{T}}}(y|x_{\mathrm{T}} = N_0). \tag{18}$$

Now, we need to obtain $P_{Y|X_{\mathrm{T}}}(y|x_{\mathrm{T}})$ from (12) and insert it into (17) and (18). To this end, we first need to find $P_{Y|X_{\mathrm{T}},X_{\mathrm{I}}}(y|x_{\mathrm{T}}, x_{\mathrm{I}})$. Since Y_{T} and Y_{I} are independent, the PMF of $Y = Y_{\mathrm{T}} + Y_{\mathrm{I}}$ can be found as a convolution of the PMFs of Y_{T} given X_{T} and the PMF of Y_{I} given X_{I}, as

$$P_Y(y) = \sum_{i=0}^{y} P_{Y_{\mathrm{T}}}(i)P_{Y_{\mathrm{I}}}(y-i). \tag{19}$$

Conditioning both sides of (19) on X_{T} and X_{I}, we obtain

$$P_{Y|X_{\mathrm{T}},X_{\mathrm{I}}}(y|x_{\mathrm{T}}, x_{\mathrm{I}}) = \sum_{i=0}^{y} P_{Y_{\mathrm{T}}|X_{\mathrm{T}},X_{\mathrm{I}}}(i|x_{\mathrm{T}}, x_{\mathrm{I}}) \times P_{Y_{\mathrm{I}}|X_{\mathrm{T}},X_{\mathrm{I}}}(y-i|x_{\mathrm{T}}, x_{\mathrm{I}}). \tag{20}$$

Now, since Y_{T} and Y_{I} are independent of X_{I} and X_{T}, respectively, (20) can be written as

$$P_{Y|X_{\mathrm{T}},X_{\mathrm{I}}}(y|x_{\mathrm{T}}, x_{\mathrm{I}}) = \sum_{i=0}^{y} P_{Y_{\mathrm{T}}|X_{\mathrm{T}}}(i|x_{\mathrm{T}})P_{Y_{\mathrm{I}}|X_{\mathrm{I}}}(y-i|x_{\mathrm{I}}). \tag{21}$$

We now have all necessary expressions to write P_{b} in (14) as a function of T_{r}. To this end, we insert the PMF expressions in (3) and (4) into (21), then insert (21) and (2) into (12), and obtain the conditional PMF $P_{Y|X_{\mathrm{T}}}(y|x_{\mathrm{T}})$. Finally, inserting $P_{Y|X_{\mathrm{T}}}(y|x_{\mathrm{T}})$ from (12) into (17) and (18) and then inserting them and (1) into (14), we derive the closed-form expression of the BER in (22), given at the bottom of the page. We note that (22) is a general expression of the BER that holds for 1D and 3D environments by substituting the corresponding distributions for p_d and $p_{d_{\mathrm{I}}}$ given in (5), (6), (7), and (8).

C. Maximum Likelihood Detection With ISI

We now relax the assumption of negligible ISI in the previous subsection and consider ML detection for a channel with memory L, i.e., the molecules received at Rx during one bit interval are released from Tx and Ix during the current and $L-1$ previous bit intervals. Since we now consider a sequence of multiple bits, we use the superscript to denote the bit interval. The total number of received molecules during the detection interval of the j-th bit is then equal to

$$Y^{(j)} = \sum_{l=0}^{L-1} Y_{\mathrm{T}}^{(j-l)} + \sum_{l=0}^{L-1} Y_{\mathrm{I}}^{(j-l)}. \tag{23}$$

$P_{Y|X_{\mathrm{T}}}(y|x_{\mathrm{T}})$ is now given by

$$P_{Y|X_{\mathrm{T}}^{(j)}}\left(y|x_{\mathrm{T}}^{(j)}\right) = \frac{1}{2^{2L-1}} \sum_{\boldsymbol{X_{\mathrm{T}}}^{(j)},\boldsymbol{X_{\mathrm{I}}}^{(j)}} P_{Y|\boldsymbol{X_{\mathrm{T}}}^{(j)},\boldsymbol{X_{\mathrm{I}}}^{(j)}}\left(y|\boldsymbol{x_{\mathrm{T}}}^{(j)}, \boldsymbol{x_{\mathrm{I}}}^{(j)}\right), \tag{24}$$

where $\boldsymbol{X_{\mathrm{T}}}^{(j)} = [X_{\mathrm{T}}^{(j-L+1)}, \ldots, X_{\mathrm{T}}^{(j)}]$, $\boldsymbol{X_{\mathrm{I}}}^{(j)} = [X_{\mathrm{I}}^{(j-L+1)}, \ldots, X_{\mathrm{I}}^{(j)}]$, and the summation in (24) is over all possible values of $\boldsymbol{X_{\mathrm{T}}}^{(j)}$ and $\boldsymbol{X_{\mathrm{I}}}^{(j)}$. $P_{Y|\boldsymbol{X_{\mathrm{T}}}^{(j)},\boldsymbol{X_{\mathrm{I}}}^{(j)}}\left(y|\boldsymbol{x_{\mathrm{T}}}^{(j)}, \boldsymbol{x_{\mathrm{I}}}^{(j)}\right)$ is given by (25) at the bottom of the page, where $*$ denotes convolution. Substituting (25) into (24), we can obtain the ML detection from (13) and the BER from (14), (17), (18), and (24), respectively.

$$P_{\mathrm{b}} = \frac{1}{4} \times \left\{ \sum_{y\in\mathbb{Z}_0} \sum_{i=0}^{y} \binom{N_1}{i} p_d^i (1-p_d)^{N_1-i} p_{d_{\mathrm{I}}}^{y-i} \left(\binom{N_0}{y-i} (1-p_{d_{\mathrm{I}}})^{N_0-(y-i)} + \binom{N_1}{y-i} (1-p_{d_{\mathrm{I}}})^{N_1-(y-i)} \right) + \sum_{y\in\mathbb{Z}_1} \sum_{i=0}^{y} \binom{N_0}{i} p_d^i (1-p_d)^{N_0-i} p_{d_{\mathrm{I}}}^{y-i} \left(\binom{N_0}{y-i} (1-p_{d_{\mathrm{I}}})^{N_0-(y-i)} + \binom{N_1}{y-i} (1-p_{d_{\mathrm{I}}})^{N_1-(y-i)} \right) \right\} \tag{22}$$

$$P_{Y|\boldsymbol{X_{\mathrm{T}}}^{(j)},\boldsymbol{X_{\mathrm{I}}}^{(j)}}\left(y|\boldsymbol{x_{\mathrm{T}}}^{(j)}, \boldsymbol{x_{\mathrm{I}}}^{(j)}\right) = P_{Y_{\mathrm{T}}^{(j)}|X_{\mathrm{T}}^{(j)}}\left(y_{\mathrm{T}}^{(j)}|x_{\mathrm{T}}^{(j)}\right) * \cdots * P_{Y_{\mathrm{T}}^{(j-L+1)}|X_{\mathrm{T}}^{(j-L+1)}}\left(y_{\mathrm{T}}^{(j-L+1)}|x_{\mathrm{T}}^{(j-L+1)}\right) * P_{Y_{\mathrm{I}}^{(j)}|X_{\mathrm{I}}^{(j)}}\left(y_{\mathrm{I}}^{(j)}|x_{\mathrm{I}}^{(j)}\right) * \cdots * P_{Y_{\mathrm{I}}^{(j-L+1)}|X_{\mathrm{I}}^{(j-L+1)}}\left(y_{\mathrm{I}}^{(j-L+1)}|x_{\mathrm{I}}^{(j-L+1)}\right) \tag{25}$$

The obtained BER expression is complicated for the ISI system and trying to optimize the BER in terms of $T_{\rm r}$ is computational expensive. Therefore, optimizing $T_{\rm r}$ assuming negligible ISI is more practical and can be considered as a suboptimal solution in the system with ISI. The performance of the systems without and with ISI using the optimal $T_{\rm r}$ obtained in the absence of ISI will be shown in Section VI.

In the above derivation of the closed-form expression of the BER for the non-ISI system, the probability $P_{Y|X_{\rm T},X_{\rm I}}(y|x_{\rm T},x_{\rm I})$ in (21) can be derived using the Binomial, Poisson, or Gaussian distribution. As explained in the introduction, the Binomial distribution describes the number of received molecules most accurately. The Poisson and Gaussian approximations are used in the literature due to their ease of analysis. In the next sections, we detail our proposed algorithms to obtain the optimal $T_{\rm r}$ according to (9) and the corresponding BER for the three distributions.

IV. Optimal Receiving Interval in a System Affected by Interference at a Known Location

In this section, we propose algorithms to obtain the optimal detection interval, $T_{\rm r}^{\star}$, that minimizes the BER of the considered system model when the location of the interference source, Ix, is known to the receiver, Rx. We consider three cases, i.e., when the Binomial, Poisson, and Gaussian distributions are used for the analysis, respectively.

A. Optimizing $T_{\rm r}$ Using the Binomial Distribution

In order to develop an algorithm to optimize $T_{\rm r}$ in terms of $P_{\rm b}$, we need the observe the property of $P_{\rm b}$ as a function of $T_{\rm r}$. From (22), we can see that $P_{\rm b}$ is not a smooth function of $T_{\rm r}$ in general, since $\mathbb{Z}_0$ and $\mathbb{Z}_1$ change discretely as $T_{\rm r}$ changes. However, the following lemma will be useful for the algorithm development.

Lemma 1: There are intervals $T_{\rm r}^{(l)} \le T_{\rm r} \le T_{\rm r}^{(l+1)}$, for $l = 1, 2, \ldots$, in which $P_{\rm b}$ is smooth with respect to $T_{\rm r}$.

Proof: Please refer to Appendix A. ∎

Given Lemma 1, we can find the optimal $T_{\rm r}$ in each of these intervals, $T_{\rm r}^{(l)} \le T_{\rm r} \le T_{\rm r}^{(l+1)}$, and obtain the corresponding minimal $P_{\rm b}$ for that interval and then compare the values of $P_{\rm b}$ from different intervals to find the global minimum. Algorithm 1 outlines our proposed iterative algorithm for finding the optimal detection interval. In particular, we first specify the sets $\mathbb{Z}_0$ and $\mathbb{Z}_1$ for $T_{\rm r}^{(l)}$ (line 4-10) and find $T_{\rm r}^{(l+1)}$ such that $\mathbb{Z}_0$ and $\mathbb{Z}_1$ are fixed for $T_{\rm r}^{(l)} \le T_{\rm r} \le T_{\rm r}^{(l+1)}$ by binary search (line 11) [51]. We then use gradient projection method (line 13-22) combined with steepest line search satisfying Armijo rule (line 23-27) [52, Sec. 6.1] to find the optimal $T_{\rm r}$ in the interval $T_{\rm r}^{(l)} \le T_{\rm r} \le T_{\rm r}^{(l+1)}$. Finally, we find the global optimal $T_{\rm r}$ by comparing optimal values of $T_{\rm r}$ in all intervals $T_{\rm r}^{(l)} \le T_{\rm r} \le T_{\rm r}^{(l+1)}$ (line 31).

Note that Algorithm 1 requires the gradient of the cost function, i.e., BER, and thus can only be used when the gradient of the BER is available. In other words, Algorithm 1 cannot be used to optimize the detection interval of the systems with ISI due to the complicated BER expressions.

Algorithm 1 Gradient Projection Method With Steepest Line Search for Optimal Detection Interval Using Binomial and Poisson Distributions

1: $k \leftarrow 0$, $t_{\rm opt}(0) \leftarrow 0$, $T_{\rm b}$, t_0, $\epsilon \to 0$, $\alpha \in (0,1)$, $\beta \in (0,1)$, $c \in (0,1)$
2: **while** $t_{\rm opt}(k) \le T_{\rm b}$ **do**
3: $\quad t_{\min} \leftarrow t_0$
4: $\quad$ **for** $y \in \{0, \ldots, 2N_1\}$ **do**
5: $\quad\quad$ **if** $P_{Y_{\rm r}|X}(y|x = N_0) > P_{Y_{\rm r}|X}(y|x = N_1)$ **then**
6: $\quad\quad\quad y \in \mathbb{Z}_0$
7: $\quad\quad$ **else**
8: $\quad\quad\quad y \in \mathbb{Z}_1$
9: $\quad\quad$ **end if**
10: $\quad$ **end for**
11: $\quad t_{\max}$:$t \le t_{\max}|\mathbb{Z}_0 \& \mathbb{Z}_1$ unchanged, $t_{\max}$ found by binary search
12: $\quad$ **while** $\|t - t_1\| \ge \epsilon$ **do**
13: $\quad\quad t \leftarrow t_1$
14: $\quad\quad$ **if** $t - \alpha \nabla P_{\rm b}(t) > t_{\max}$ **then**
15: $\quad\quad\quad d \leftarrow t_{\max} - t$
16: $\quad\quad$ **else**
17: $\quad\quad\quad$ **if** $t - \alpha \nabla P_{\rm b}(t) < t_{\min}$ **then**
18: $\quad\quad\quad\quad d \leftarrow t_{\min} - t$
19: $\quad\quad\quad$ **else**
20: $\quad\quad\quad\quad d \leftarrow -\alpha \nabla P_{\rm b}(t)$
21: $\quad\quad\quad$ **end if**
22: $\quad\quad$ **end if**
23: $\quad\quad m \leftarrow 0$
24: $\quad\quad$ **while** $P_{\rm b}(t) - P_{\rm b}(t + \beta^m d) < -c\beta^m \nabla P_{\rm b}(t) d$ **do**
25: $\quad\quad\quad m \leftarrow m + 1$
26: $\quad\quad$ **end while**
27: $\quad\quad t_1 \leftarrow t + \beta^m d$
28: $\quad$ **end while**
29: $\quad t_{\rm opt}(k) \leftarrow t_1$, $k \leftarrow k + 1$, $t_0 \leftarrow t_{\max}$
30: **end while**
31: $t^{\star} \leftarrow \min(t_{\rm opt})$

B. Approximation of the Optimal $T_{\rm r}$ Using the Poisson Distribution

When the number of released molecules is very large, i.e., $X_{\rm T} \gg 1$ and $X_{\rm I} \gg 1$ hold, the Binomial distributions of $Y_{\rm T}$ and $Y_{\rm I}$ conditioned on $X_{\rm T}$ and $X_{\rm I}$, respectively, can be approximated by Poisson distributions as $Y_{\rm T} \sim \mathsf{Poiss}(X_{\rm T} p_d)$ and $Y_{\rm I} \sim \mathsf{Poiss}(X_{\rm I} p_{d_{\rm I}})$ [20].

Now, due to the fact that the sum of two Poisson random variables also follows a Poisson distribution, we have $Y \sim \mathsf{Poiss}(X_{\rm T} p_d + X_{\rm I} p_{d_{\rm I}})$. Therefore,

$$P_{Y|X_{\rm T},X_{\rm I}}(y|x_{\rm T},x_{\rm I}) = \frac{\left(x_{\rm T} p_d + x_{\rm I} p_{d_{\rm I}}\right)^y e^{-\left(x_{\rm T} p_d + x_{\rm I} p_{d_{\rm I}}\right)}}{y!}. \tag{26}$$

Inserting (26) and (2) into (12), then inserting (12) into (17), (18), and then inserting them and (1) into (14), we obtain a closed-form expression for the BER in (27) given at the bottom

of the page, where p_d and p_{d_I} are given respectively by (5) and (6) for a 1D system, or (7) and (8) for a 3D system.

Since the Poisson distribution is discrete, we can use Algorithm 1 to find the optimal T_r.

C. Approximation of the Optimal T_r Using the Gaussian Distribution

Since $X_\mathrm{T} \gg 1$ and $X_\mathrm{I} \gg 1$ hold, the Binomial distributions of Y_T and Y_I conditioned on X_T and X_I, respectively, can also be approximated by Gaussian distributions as $Y_\mathrm{T} \sim \mathcal{N}(X_\mathrm{T} p_d, X_\mathrm{T} p_d(1-p_d))$ and $Y_\mathrm{I} \sim \mathcal{N}(X_\mathrm{I} p_{d_\mathrm{I}}, X_\mathrm{I} p_{d_\mathrm{I}}(1-p_{d_\mathrm{I}}))$ [20]. In this case, since the sum of two Gaussian random variables is also a Gaussian random variable, we have $Y \sim \mathcal{N}(X_\mathrm{T} p_d + X_\mathrm{I} p_{d_\mathrm{I}}, X_\mathrm{T} p_d(1-p_d) + X_\mathrm{I} p_{d_\mathrm{I}}(1-p_{d_\mathrm{I}}))$ and

$$P_{Y|X_\mathrm{T},X_\mathrm{I}}(y|x_\mathrm{T},x_\mathrm{I}) = \frac{1}{\sqrt{2\pi\big(x_\mathrm{T} p_d(1-p_d) + x_\mathrm{I} p_{d_\mathrm{I}}\big(1-p_{d_\mathrm{I}}\big)\big)}} \times \exp\left(-\frac{\big(y-\big(x_\mathrm{T} p_d + x_\mathrm{I} p_{d_\mathrm{I}}\big)\big)^2}{2\big(x_\mathrm{T} p_d(1-p_d) + x_\mathrm{I} p_{d_\mathrm{I}}\big(1-p_{d_\mathrm{I}}\big)\big)}\right). \quad (28)$$

Then, $P_{Y|X_\mathrm{T}}(y|x_\mathrm{T})$ is found by inserting (28) and (2) into (12). Note that, $P_{Y|X_\mathrm{T},X_\mathrm{I}}(y|x_\mathrm{T},x_\mathrm{I})$ and $P_{Y|X_\mathrm{T}}(y|x_\mathrm{T})$ are now continuous functions with respect to Y since Y follows the Gaussian distribution. Therefore, $\mathbb{Z}_0$ and $\mathbb{Z}_1$, and the BER now have to be derived differently than when Y is discrete.

Since the set $\mathbb{Z}_k$, for $k \in \{0,1\}$ is now a continuous set, we can present $\mathbb{Z}_0$ and $\mathbb{Z}_1$ as a combination of the ranges $[\gamma_i, \gamma_{i+1}]$, where i is even for $k=0$ and i is odd for $k=1$, and γ_i and γ_{i+1} are lower and upper bounds of the range i. Then, from (10), we have $P_{Y|X_\mathrm{T}}(y|x_\mathrm{T}=N_0) > P_{Y|X_\mathrm{T}}(y|x_\mathrm{T}=N_1)$ when y belongs to $[\gamma_i, \gamma_{i+1}]$ and i is even. Similarly, $P_{Y|X_\mathrm{T}}(y|x_\mathrm{T}=N_1) \geq P_{Y|X_\mathrm{T}}(y|x_\mathrm{T}=N_0)$ holds when y belongs to $[\gamma_i, \gamma_{i+1}]$ and i is odd. Therefore, γ_i, for $i = 0, 1, 2, \ldots$ are found by numerically solving the following equation

$$P_{Y|X_\mathrm{T}}(y|x_\mathrm{T}=N_1) = P_{Y|X_\mathrm{T}}(y|x_\mathrm{T}=N_0). \quad (29)$$

The closed-form expression of the BER for this case is given in (30) at the bottom of the next page, where p_d and p_{d_I} are given respectively by (5) and (6) for a 1D system, or (7) and (8) for a 3D system (see Appendix B for the detailed derivation). Since the bounds γ_i, for $i = 0, 1, 2, \ldots$, of set $\mathbb{Z}_0$ and set $\mathbb{Z}_1$ are found by numerically solving (29), i.e., there is no closed-form expression of γ_i, deriving the derivative of the BER function does not lead to an insightful expression that can be used in Algorithm 1. Therefore, we use implicit filtering [53] to find the optimal detection interval, $T_\mathrm{r}^\star$, that minimizes the BER given in (30) as outlined in Algorithm 2. In particular, we use implicit filtering [53, Algorithm 9.6] combined with projection (line 10 and 13) to ensure the new value of T_r is within the range $[0, T_\mathrm{b}]$.

Algorithm 2 Implicit Filtering Algorithm for Optimal Detection Interval Using the Gaussian Distribution

1: T_b, $a_{\max}$, $\epsilon \to 0$, $\tau \to 0$ $\alpha \in (0,1)$, $\beta \in (0,1)$, $c \in (0,1)$
2: **while** $\epsilon \geq \tau$ **do**
3: $\quad increment \leftarrow 0$
4: $\quad$ **while** $increment = 0$ **do**
5: $\quad\quad g \leftarrow (P_\mathrm{b}(t+\epsilon) - P_\mathrm{b}(t+\epsilon))/(2\epsilon)$
6: $\quad\quad$ **if** $\|g\| \leq \epsilon$ **then**
7: $\quad\quad\quad increment \leftarrow 1$
8: $\quad\quad$ **else**
9: $\quad\quad\quad m \leftarrow 1$
10: $\quad\quad\quad d \leftarrow \mathbf{P}_{[0,T_\mathrm{b}]}(t - \rho^m g)$ (Projection of $t - \rho^m g$ on the value range of T_r, $[0, T_\mathrm{b}]$)
11: $\quad\quad\quad$ **while** $P_\mathrm{b}(d) > P_\mathrm{b}(t) - \alpha\beta^m g^2$ and $m < a_{\max}$ **do**
12: $\quad\quad\quad\quad m \leftarrow m + 1$
13: $\quad\quad\quad\quad d \leftarrow \mathbf{P}_{[0,T_\mathrm{b}]}(t - \beta^m g)$ (Projection of $t - \beta^m g$ on the value range of T_r, $[0, T_\mathrm{b}]$)
14: $\quad\quad\quad$ **end while**
15: $\quad\quad\quad$ **if** $m = a_{\max}$ **then**
16: $\quad\quad\quad\quad increment \leftarrow 1$
17: $\quad\quad\quad$ **else**
18: $\quad\quad\quad\quad t = d$
19: $\quad\quad\quad$ **end if**
20: $\quad\quad$ **end if**
21: $\quad$ **end while**
22: $\quad \epsilon \leftarrow \epsilon c$
23: **end while**

Remark 2: In general, the Poisson approximation is more accurate than the Gaussian approximation when p_d and p_{d_I} are close to one or zero [23], [54]. In other cases, i.e., when p_d and p_{d_I} are not close to one or zero, the Gaussian approximation is more accurate than the Poisson approximation. In practice, to keep the reliability of the system high, we must not design the system with p_d close to zero, i.e., receiving very few information molecules, or p_{d_I} close to one, i.e., receiving too many interference molecules. Therefore, the Gaussian approximation may be more accurate in these designs despite the fact that Poisson approximation can capture the discreteness and non-negativity of the counting variable.

Remark 3: The optimal T_r given by Algorithm 1 is a global optimum. Since the Binomial distribution is approximated by the Poisson and the Gaussian distributions, the three distributions result in similar behaviors of the BER (shown in the numerical section). Therefore, we give proof for the global optimum of T_r only for the case of the Poisson distribution (See Appendix C).

$$P_{\mathrm{b,Poisson}} = \frac{1}{4}\left\{\sum_{y\in\mathbb{Z}_0}\left(\frac{\big(N_1 p_d + N_0 p_{d_\mathrm{I}}\big)^y e^{-\left(N_1 p_d + N_0 p_{d_\mathrm{I}}\right)}}{y!} + \frac{\big(N_1 p_d + N_1 p_{d_\mathrm{I}}\big)^y e^{-\left(N_1 p_d + N_1 p_{d_\mathrm{I}}\right)}}{y!}\right) + \sum_{y\in\mathbb{Z}_1}\left(\frac{\big(N_0 p_d + N_0 p_{d_\mathrm{I}}\big)^y e^{-\left(N_0 p_d + N_0 p_{d_\mathrm{I}}\right)}}{y!} + \frac{\big(N_0 p_d + N_1 p_{d_\mathrm{I}}\big)^y e^{-\left(N_0 p_d + N_1 p_{d_\mathrm{I}}\right)}}{y!}\right)\right\} \quad (27)$$

Remark 4: In order to optimize the detection interval, we proposed suitable algorithms according to the properties of the optimization problems. In particular, Algorithm 1 and 2 handle the lack of the function smoothness and of the function derivative, respectively. The optimization process using these algorithms can be done offline and the result can then be used to set the optimal duration of the detection interval at the receiver. Hence, there is no complex calculation required in the MC systems yet system performance is improved by the proposed optimal design.

V. Optimal Receiving Interval in a System Affected by Interference at an Unknown Location

In this section, we generalize the investigation of the 1D system and consider that the exact location of the interference source Ix is unknown to the receiver Rx. Instead, the receiver has only statistical knowledge of the location.

We assume that the interference source is randomly located between distances a and b from the receiver according to the uniform distribution. Thereby, the distance $d_{\rm I}$ from the receiver to the interference source, Ix, is now a random variable following the uniform distribution, i.e., $d_{\rm I} \sim \boldsymbol{\mathcal{U}}(a,b)$. Since the receiver does not know $d_{\rm I}$, the detection process is optimal when the receiver uses maximum likelihood of the expectation of the PMF of the number of received molecules, as follows

$$\begin{aligned}\hat{X} &= \underset{X_{\rm T}\in\{N_0,N_1\}}{\arg\max}\ \mathbb{E}_{d_{\rm I}}\Big[P_{Y|X_{\rm T}}(\,y|x_{\rm T})\Big] \\ &= \underset{X_{\rm T}\in\{N_0,N_1\}}{\arg\max}\int_a^b \frac{1}{b-a}P_{Y|X_{\rm T}}(\,y|x_{\rm T})\,dd_{\rm I}, \end{aligned} \tag{31}$$

where $P_{Y|X_{\rm T}}(\,y|x_{\rm T})$ is given as in Section IV for each corresponding distribution and $\mathbb{E}[.]$ denotes the expectation.

For the detection rule in this case, we redefine $\mathbb{Z}_0$ and $\mathbb{Z}_1$ as the sets of numbers of received molecules for which $\mathbb{E}_{d_{\rm I}}[P_{Y|X_{\rm T}}(\,y|x_{\rm T}=N_0)]$ is larger than $\mathbb{E}_{d_{\rm I}}[P_{Y|X_{\rm T}}(\,y|x_{\rm T}=N_1)]$ and vice versa, respectively, when $0 \le y \le 2N_1$. For both the Binomial and Poisson distributions, $\mathbb{Z}_0$ and $\mathbb{Z}_1$ can be found by comparing $\mathbb{E}_{d_{\rm I}}[P_{Y|X_{\rm T}}(\,y|x_{\rm T}=N_0)]$ and $\mathbb{E}_{d_{\rm I}}[P_{Y|X_{\rm T}}(\,y|x_{\rm T}=N_1)]$. On the other hand, for Gaussian distribution, $\mathbb{Z}_0$ and $\mathbb{Z}_1$ can be found by numerically solving the following equation

$$\int_a^b P_{Y|X_{\rm T}}(\,y|x_{\rm T}=N_0)\,dd_{\rm I} = \int_a^b P_{Y|X_{\rm T}}(\,y|x_{\rm T}=N_1)\,dd_{\rm I}. \tag{32}$$

TABLE I
Parameters of the Systems Used for Numerical Results

Parameter	Value	Parameter	Value
D [m^2/s]	10^{-9}	r [m]	1×10^{-6}
d [m]	1.5×10^{-5}	$d_{\rm I}$ [m]	6×10^{-5}
$T_{\rm b}$[s](1D)	7.12	$T_{\rm b}$[s](3D)	6.21
$N_0 = M_0(1D)$	20	$N_1 = M_1(1D)$	40
$N_0 = M_0(3D)$	1000	$N_1 = M_1(3D)$	2000

Furthermore, from (31), we have

$$\begin{aligned}&P_{\hat{X}_{\rm T}|X_{\rm T}}(\,\hat{x}_{\rm T}=N_0|x_{\rm T}=N_1) \\ &\quad=\sum_{y\in\mathbb{Z}_0}\int_a^b \frac{1}{b-a}P_{Y|X_{\rm T}}(\,y|x_{\rm T}=N_1)\,dd_{\rm I}\end{aligned} \tag{33}$$

and

$$\begin{aligned}&P_{\hat{X}_{\rm T}|X_{\rm T}}(\,\hat{x}_{\rm T}=N_1|x_{\rm T}=N_0) \\ &\quad=\sum_{y\in\mathbb{Z}_1}\int_a^b \frac{1}{b-a}P_{Y|X_{\rm T}}(\,y|x_{\rm T}=N_0)\,dd_{\rm I}.\end{aligned} \tag{34}$$

Therefore, using similar derivation as in Section IV with $P_{\hat{X}_{\rm T}|X_{\rm T}}$ given by (33) and (34), we can obtain the BER $P'_{\rm b}$ of the system affected by interference at an unknown location as follows

$$P'_{\rm b} = \int_a^b \frac{1}{b-a}P_{\rm b}\,dd_{\rm I}. \tag{35}$$

Note that (35) holds for the corresponding BER for Binomial, Poisson, and Gaussian distributions.

We can use the algorithms developed in Section IV to find the optimal detection interval when Binomial, Poisson, and Gaussian distributions are used, respectively.

Note that the results in this section can be extended to the 3D case. In that case, the derivation in (31)–(35) needs to evaluate the integration over the 3D space that the interference is located in, instead of the 1D integral.

VI. Numerical Results

In this section, we illustrate the dependence of the BER on the detection interval $T_{\rm r}$ and show the impacts of optimizing $T_{\rm r}$ on the BER. Unless otherwise stated, we use the default values of the parameters given in Table I, which are in the same orders of commonly-used values in the literature [2], [7], [46]. In an unbounded 3D environment, larger amounts of

$$\begin{aligned}P_{\rm b,Gaussian} = \frac{1}{8}\Bigg(&\sum_{i=0,2,\ldots}\Bigg(\operatorname{erf}\Bigg(\frac{\gamma_{i+1}-\big(N_1p_d+N_0p_{d_{\rm I}}\big)}{N_1p_d(1-p_d)+N_0p_{d_{\rm I}}(1-p_{d_{\rm I}})}\Bigg)-\operatorname{erf}\Bigg(\frac{\gamma_i-\big(N_1p_d+N_0p_{d_{\rm I}}\big)}{N_1p_d(1-p_d)+N_0p_{d_{\rm I}}(1-p_{d_{\rm I}})}\Bigg)\\ &+\operatorname{erf}\Bigg(\frac{\gamma_{i+1}-\big(N_1p_d+N_1p_{d_{\rm I}}\big)}{N_1p_d(1-p_d)+N_1p_{d_{\rm I}}(1-p_{d_{\rm I}})}\Bigg)-\operatorname{erf}\Bigg(\frac{\gamma_i-\big(N_1p_d+N_1p_{d_{\rm I}}\big)}{N_1p_d(1-p_d)+N_1p_{d_{\rm I}}(1-p_{d_{\rm I}})}\Bigg)\Bigg)\\ &+\sum_{i=1,3,\ldots}\Bigg(\operatorname{erf}\Bigg(\frac{\gamma_{i+1}-\big(N_0p_d+N_0p_{d_{\rm I}}\big)}{N_0p_d(1-p_d)+N_0p_{d_{\rm I}}(1-p_{d_{\rm I}})}\Bigg)-\operatorname{erf}\Bigg(\frac{\gamma_i-\big(N_0p_d+N_0p_{d_{\rm I}}\big)}{N_0p_d(1-p_d)+N_0p_{d_{\rm I}}(1-p_{d_{\rm I}})}\Bigg)\\ &+\operatorname{erf}\Bigg(\frac{\gamma_{i+1}-\big(N_0p_d+N_1p_{d_{\rm I}}\big)}{N_0p_d(1-p_d)+N_1p_{d_{\rm I}}(1-p_{d_{\rm I}})}\Bigg)-\operatorname{erf}\Bigg(\frac{\gamma_i-\big(N_0p_d+N_1p_{d_{\rm I}}\big)}{N_0p_d(1-p_d)+N_1p_{d_{\rm I}}(1-p_{d_{\rm I}})}\Bigg)\Bigg)\Bigg)\end{aligned} \tag{30}$$

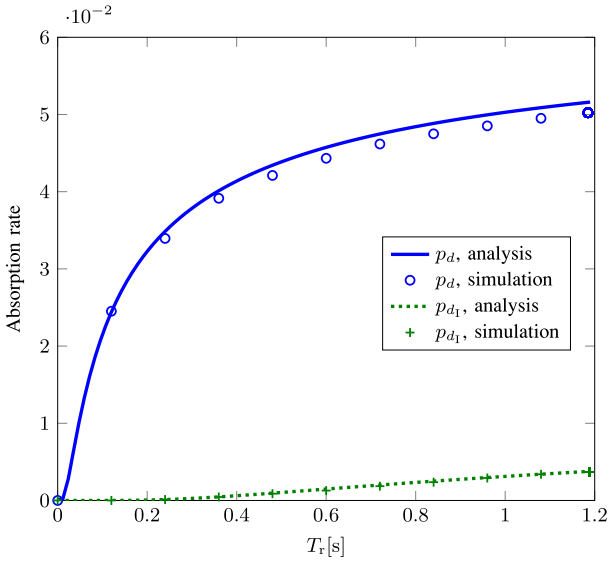

Fig. 3. Absorption rates, p_d and $p_{d_{\mathrm{I}}}$, as a function of T_{r} when there are two pairs of transceivers in a 3D MC system.

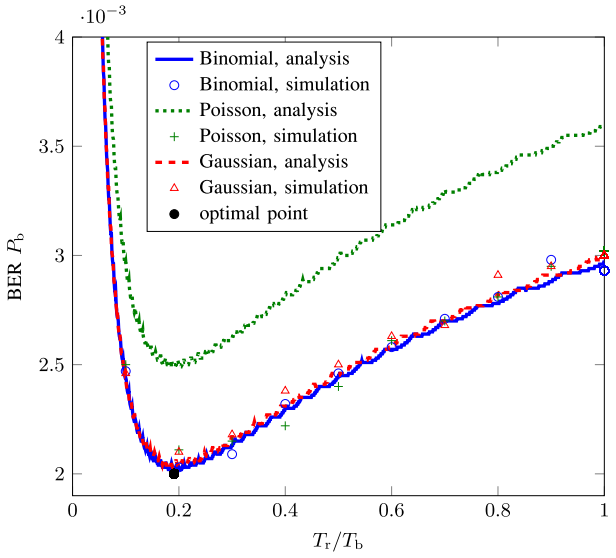

Fig. 4. BER as a function of $T_{\mathrm{r}}/T_{\mathrm{b}}$ in a 3D system affected by interference when the number of received molecules is described by a Binomial distribution and approximated by Poisson and Gaussian distributions.

molecules, i.e., N and M, are needed since the molecules diffuse in all dimensions and only a small portion of them can reach the receiver. For the system parameters in Table I, to ensure that the ISI caused by the Tx is small, T_{b} is chosen such that the ratio between p_d with $T_{\mathrm{r}} = T_{\mathrm{b}}$ to p_d with $T_{\mathrm{r}} \to \infty$ is equal to 90% [26]. In particular, from $\frac{p_d(T_{\mathrm{r}}=T_{\mathrm{b}})}{p_d(T_{\mathrm{r}}=\infty)} = 0.9$, (5), and (7), we have $T_{\mathrm{b}} = d^2/(4D\mathrm{erfcinv}^2(0.9)) = 7.12$s for a 1D system and $T_{\mathrm{b}} = (d-r)^2/(4D\mathrm{erfcinv}^2(0.9)) = 6.21$s for a 3D system, where $\mathrm{erfcinv}(\cdot)$ is the inverse complementary error function. Eliminating interference caused by the Ix will be taken into account in the design of the optimal detection interval. For smaller d, the ISI caused by the Tx will be higher compared to the default value of d in Table I. We will highlight in our results that the design of the optimal detection interval to eliminate interference from Ix is still valid for the performance improvement of the system with ISI. Unless otherwise stated, the value of T_{b} is fixed in order to investigate the impact of T_{r}. The detection interval is optimized with the assumption of no ISI. However, the performance of systems with ISI is also shown numerically. For Fig. 3, we adopt the particle-based simulation of Brownian motion, where the molecules take a random step in space for every discrete time step of length $\Delta t = 10^{-5}$s. The length of each step in each spatial dimension is modeled as a Gaussian random variable with zero mean and standard deviation $\sqrt{2D\Delta t}$. In the other simulation, we adopt Monte-Carlo simulation by averaging the BER over 10^5 transmissions. In particular, we generate released molecules according to the modulation rule, counting the number of molecules absorbed during the detection interval. Then, the decoded bit is decided by comparing whether the number of received molecules Y belongs to the set $\mathbb{Z}_0$ or $\mathbb{Z}_1$, as in (13).

In Fig. 3, we consider a 3D MC system with two pairs of transceivers to present the case when the impact of an absorbing receiver on the other is not significant and thus verify our assumption. In Fig. 3, we plot p_d and $p_{d_{\mathrm{I}}}$ as functions of the detection interval T_{r} with analytical expressions given in (7) and (8), respectively. We observe that p_d given by (7) matches the simulation points. We also observe an exact match for $p_{d_{\mathrm{I}}}$.

Fig. 4 shows the BER of a 3D system as a function of the ratio of the detection interval, T_{r}, to the transmission symbol interval, T_{b}, when the number of received molecules is described by the Binomial distribution and when it is approximated by Poisson and Gaussian distributions. As can be seen from Fig. 4, the BER in the system affected by external interference does not decrease monotonically when T_{r} increases. Thereby the optimal detection interval, $T_{\mathrm{r}}^{\star}$, that minimizes the BER is usually not equal to the transmission symbol interval, T_{b}. In fact, when T_{r} increases and T_{b} is constant, the BER decreases to a minimum value and then increases. The minimum value of the BER matches with the BER of the optimal T_{r} found by Algorithm 1, i.e., the black dot in Fig. 4. The dependence of the BER on T_{r} can be explained as follows. When $T_{\mathrm{r}} = 0, P_{\mathrm{b}} = 0.5$ since there are no received molecules at the Rx. As T_{r} increases, more molecules from Tx are received at the Rx and thus the BER decreases from the maximum of 0.5 when $T_{\mathrm{r}}/T_{\mathrm{b}} = 0$ and reaches a minimum value of 2×10^{-3} when $T_{\mathrm{r}}/T_{\mathrm{b}} = 0.2$. When T_{r} increases even more, more transmitted molecules from Tx and Ix are received and the impact of molecules from Ix becomes more significant. Therefore, the BER increases. Moreover, we observe a mismatch between the analysis results with Poisson distribution and other results since Poisson is only an accurate approximation when p_d and $p_{d_{\mathrm{I}}}$ are close to 0 or 1 [54]. The simulation results are in agreement since we generate the number of received molecules following the true Binomial distribution and only use the approximated distribution for detection designs. However, the analytical results for the Poisson distribution display similar characteristics with other results as a function of $T_{\mathrm{r}}/T_{\mathrm{b}}$, i.e., has the same minimum point.

In Fig. 5, the ratio of the optimal detection interval, $T_{\mathrm{r}}^{\star}$, to a fixed transmission symbol interval, T_{b}, is shown as a function of the ratio of d_{I} to a fixed d for a 1D system without ISI using the Binomial distribution and the Poisson and Gaussian

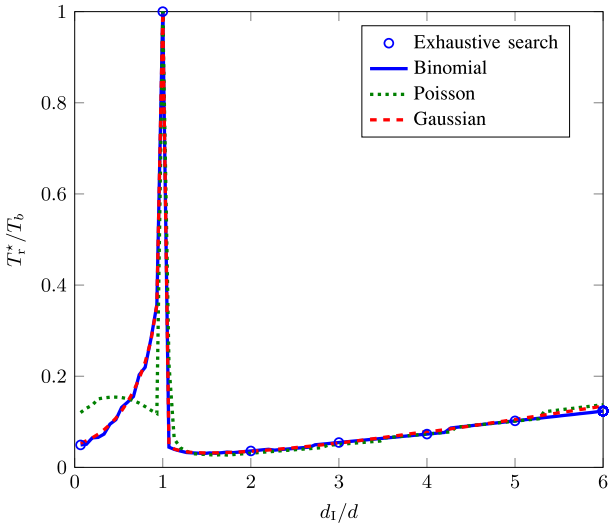

Fig. 5. The ratio of the optimal detection interval, $T_r^\star$, to the transmission symbol interval, T_b, as a function of the ratio of d_I to d in a 1D system when using the Binomial distribution, and Poisson and Gaussian approximations.

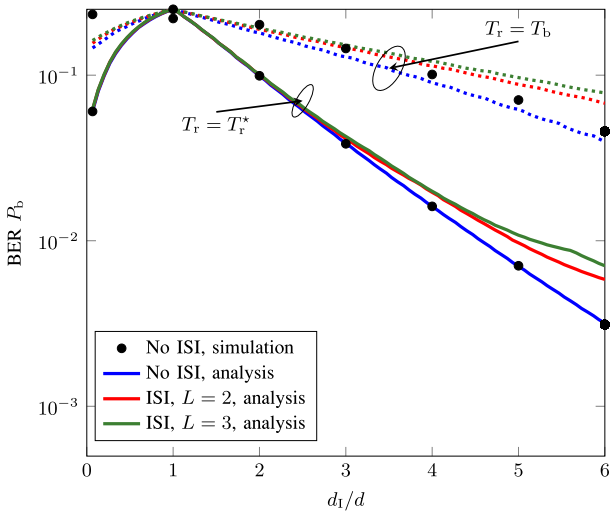

Fig. 6. The BER of a 1D system as a function of the ratio of d_I to d when T_r is optimized and when $T_r = T_b$. The systems with ISI use the optimal T_r designed for the non-ISI system.

approximations. It is observed from Fig. 5 that the optimal detection interval can be very short compared to the transmission symbol interval. When Rx is much closer to Ix than to Tx, i.e., $d_I < d$, a large T_r allows more molecules from Ix to be counted for the detection so $T_r^\star$ should be much smaller than T_b. Even when Rx is closer to Tx than to Ix, i.e., $d < d_I$, but Ix is still close to Rx, i.e., d_I is small, $T_r^\star$ should be much smaller than T_b to avoid molecules from Ix. When Ix is farther from Rx, i.e., d_I increases, $T_r^\star$ becomes larger. When Ix is very far from Rx as if it does not exist, we should have $T_r = T_b$ so that more molecules, which are only from Tx, are counted for a more accurate detection. Moreover, when $d_I \approx d$, $T_r = T_b$ is a good choice because molecules from Tx and Ix arrive at the receiver with equal probabilities and cannot be distinguished. Hence, taking all molecules into account can be helpful for the detection. Furthermore, we observe that the proposed algorithms accurately evaluates the global optimum since the optimal detection intervals, $T_r^\star$, found by exhaustive search (shown by circle markers) match $T_r^\star$ obtained by the algorithms. Only when $d_I < d$, the results for Poisson distribution are different from other results since p_{d_I} is large and the Poisson approximation is not accurate as explained in the discussion of Fig. 4.

In Fig. 6, we compare the BERs of 1D systems affected by external interference when T_r is optimal, i.e., $T_r = T_r^\star$, and when $T_r = T_b$. In particular, $T_r^\star$ is designed for the system without ISI and the BERs of the systems without ISI are presented. Moreover, the BERs of the systems with ISI, $L = 2$ or $L = 3$, using $T_r^\star$ and $T_r = T_b$ are also presented. From Fig. 6, we observe that when $T_r = T_b$, the BER, P_b, is much higher than the BER for $T_r = T_r^\star$. The decrease in the BER for optimal T_r is more significant when the interference source is far away from the transmitter. $P_b = 0.25$ when $d_I = d$ since information and interference molecules cannot be distinguished. The simulation result confirms the analysis. Moreover, Fig. 6 shows that the BERs of the systems with ISI are higher than that of the system without ISI, as expected.

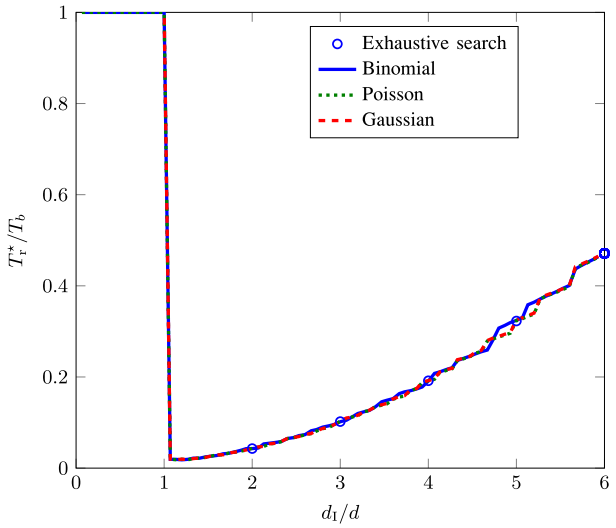

Fig. 7. The ratio of the optimal detection interval, $T_r^\star$, to the transmission symbol interval, T_b, as a function of the ratio of d_I to d in a 3D system when using Binomial distribution, and Poisson and Gaussian approximations.

However, when the systems with ISI use $T_r^\star$ designed for the non-ISI system, their BERs are also reduced compared to the BER when using $T_r = T_b$. The reduction of BER due to the $T_r^\star$ in the system with ISI is as significant as that in the system without ISI, for example, 10 time reduction when $d_I/d = 6$.

Fig. 7 shows the ratio of the optimal detection interval, $T_r^\star$, to a fixed transmission symbol interval, T_b, as a function of the ratio of d_I to a fixed d for the 3D system without ISI using Binomial distribution and the Poisson and Gaussian approximations. We observe from Fig. 7 that $T_r^\star$ can be much smaller than T_b when Tx is closer to Rx than Ix, i.e., $d < d_I$. The reason is similar to the 1D system, i.e., $T_r^\star$ should be smaller than T_b so that fewer molecules from Ix are counted for the detection. However, when $d_I \leq d$, $T_r^\star$ should be equal to T_b, which is different from the 1D system. The reason is that in a 3D system, p_d and p_{d_I} are very small compared to the 1D system with the same parameters, which means even

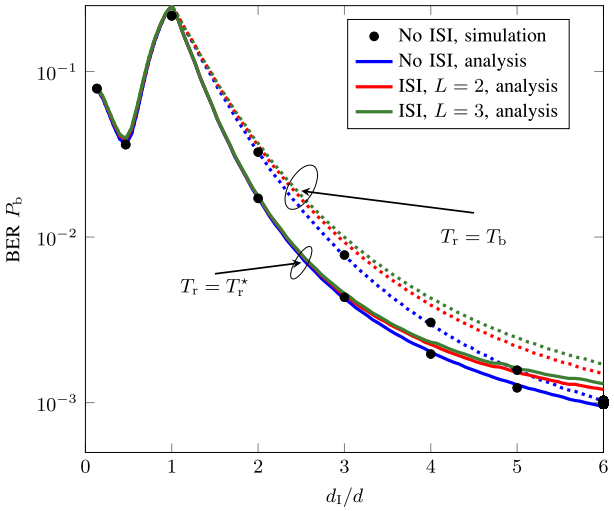

Fig. 8. The BER of a 3D system as a function of the ratio of d_I to d when T_r is optimized and when $T_\mathrm{r} = T_\mathrm{b}$, for ISI and no ISI.

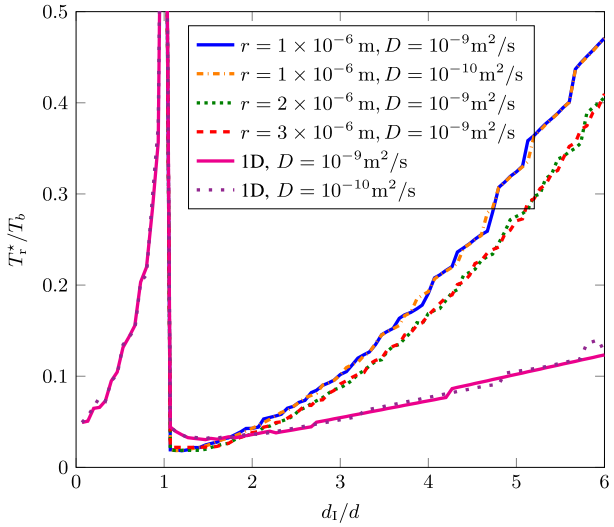

Fig. 9. The ratio of the optimal detection interval, $T_\mathrm{r}^\star$, to the transmission symbol interval, T_b, as a function of the ratio of d_I to d in 1D and 3D systems with different D and r and no ISI.

when T_r increases to infinity, all of the molecules cannot be received. Therefore, when $d_\mathrm{I} \leq d$, $T_\mathrm{r} = T_\mathrm{b}$ holds such that more molecules from the Tx can arrive for the detection, with the compromise of receiving more molecules from Ix. Moreover, the exhaustive search provides the same optimal T_r as $T_\mathrm{r}^\star$ given by the proposed algorithms. Poisson and Gaussian approximations give similar results to Binomial distribution since p_d and p_{d_I} are small in 3D systems.

Fig. 8 shows the BER as a function of d_I/d when $T_\mathrm{r} = T_\mathrm{r}^\star$ and $T_\mathrm{r} = T_\mathrm{b}$ for 3D systems without ISI and with ISI, i.e., $L = 2$ or $L = 3$. Note that $T_\mathrm{r}^\star$ is optimized for the system without ISI. In Fig. 8, we observe the improvement in the performance of systems with and without ISI in terms of BER by optimizing T_r compared to when $T_\mathrm{r} = T_\mathrm{b}$. The improvement is significant when Ix is not too close or too far from Tx, e.g., $d_\mathrm{I}/d = 3$. If Ix is far from Tx, molecules from Ix may not reach Rx and thus $T_\mathrm{r}^\star$ approaches T_b, as shown in Fig. 7, and the improvement is not significant. If Ix is close to Tx, more molecules from Ix are received and thus optimizing T_r is not helpful. Obviously, when $d_\mathrm{I} \leq d$, $T_\mathrm{r}^\star = T_\mathrm{b}$ and thus there is no improvement in the BER.

Fig. 9 shows the ratio of the optimal detection interval, $T_\mathrm{r}^\star$, to a transmission symbol interval, T_b, as a function of the ratio of d_I to a fixed d for the 1D and 3D systems with $D = \{10^{-9}, 10^{-10}\}$m^2/s and $r = \{1, 2, 3\} \times 10^{-6}$ m and no ISI. T_b is fixed when d_I varies but changes for different D and r so that the ratio between p_d with $T_\mathrm{r} = T_\mathrm{b}$ to p_d with $T_\mathrm{r} \to \infty$ is equal to 90%. Due to (5), (7), and the way T_b is chosen, DT_b remains constant when D changes. Hence, p_d and p_{d_I}, for $T_\mathrm{r} = T_\mathrm{b}$ and $T_\mathrm{r} = T_\mathrm{r}^\star$, do not change when D changes. Therefore, in both 1D and 3D systems, for different D, the ratio $T_\mathrm{r}^\star/T_\mathrm{b}$ and the BER do not change as shown in Figs. 9 and 10, respectively. When r increases in 3D systems, p_d and p_{d_I} change and thus T_b and $T_\mathrm{r}^\star$ decrease differently due to (5) and (7). Hence, the ratio $T_\mathrm{r}^\star/T_\mathrm{b}$ may not change or change insignificantly, as shown in Fig. 9. However, with different system parameters, we still observe in Fig. 9 that $T_\mathrm{r}^\star$ can be much smaller than T_b when $d < d_\mathrm{I}$, as previously shown in

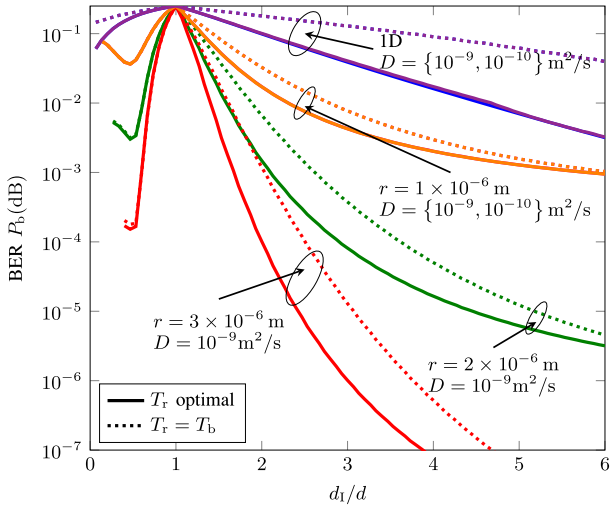

Fig. 10. The BER of a 3D system as a function of the ratio of d_I to d when T_r is optimized and when $T_\mathrm{r} = T_\mathrm{b}$, in 1D and 3D systems with different D and r and no ISI.

Figs. 5 and 7. In Fig. 10, we observe significant improvement in the BER of the systems with $T_\mathrm{r} = T_\mathrm{r}^\star$ compared to that of the systems with $T_\mathrm{r} = T_\mathrm{b}$ for different simulation parameters. In particular, for 3D systems, the BER improvement is more significant when r increases, i.e., when the BER is small. For example, when $d_\mathrm{I}/d = 3$, BER is improved by approximately twice, four times, and ten times for $r = \{1, 2, 3\} \times 10^{-6}$ m, respectively.

Fig. 11 shows the BER of 3D systems with ISI using the detection that assumes $L = 2$ or $L = 7$ as a function of T_b for $T_\mathrm{r} = T_\mathrm{r}^\star$ and $T_\mathrm{r} = T_\mathrm{b}$. $T_\mathrm{r}^\star$ is obtained by assuming no ISI in the system. The results are obtained by simulation. We consider 1000 sequences whose length is 100 symbols and ISI happens in the whole sequence. For a practical detection, the ML detections assume only ISI from one and six previous symbols, i.e., $L = 2$ and $L = 7$, respectively. In Fig. 11, we observe that when T_b is small, ISI dominates the inference from Ix and BER is high. Hence, in this case, optimizing T_r

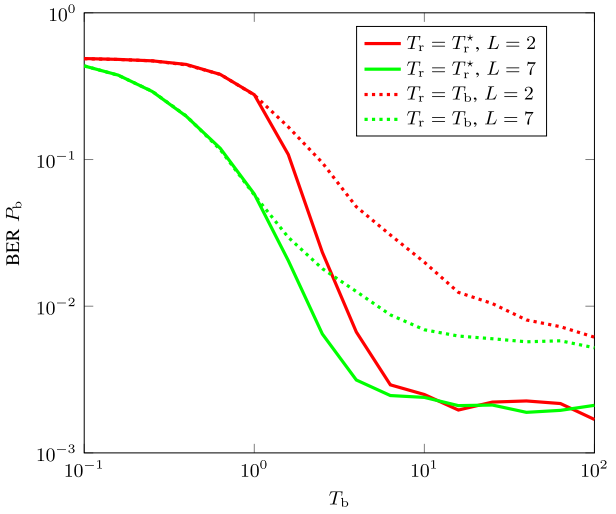

Fig. 11. The BER of 3D systems with ISI using the detection that assumes $L = 2$ or $L = 7$ for $T_{\mathrm{r}} = T_{\mathrm{r}}^{\star}$ and $T_{\mathrm{r}} = T_{\mathrm{b}}$.

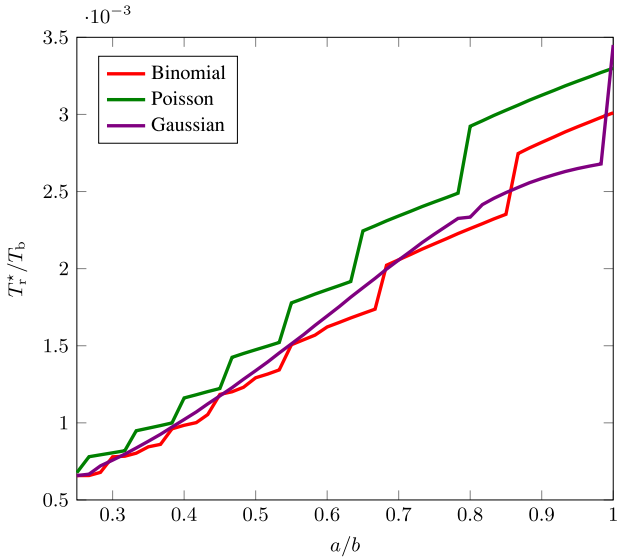

Fig. 12. The ratio of the optimal detection interval, $T_{\mathrm{r}}^{\star}$, to the transmission symbol interval, T_{b}, as a function of a/b in a 1D system with unknown-location interference.

cannot improve the system performance. However, the BER of systems with ISI reduces significantly for $T_{\mathrm{r}} = T_{\mathrm{r}}^{\star}$ compared to $T_{\mathrm{r}} = T_{\mathrm{b}}$ when T_{b} is large, even though $T_{\mathrm{r}}^{\star}$ is optimized for the system without ISI. This is because ISI impact decreases when T_{b} increases. This confirms the benefit of the proposed optimal detection interval even in systems with ISI.

Fig. 12 presents the ratio of the optimal detection interval, $T_{\mathrm{r}}^{\star}$, to the transmission symbol interval, T_{b}, as a function of a/b, when the interference source is distributed uniformly between distances a and b from the receiver. Since the uncertain position of Ix reduces the system performance, we consider that Ix is far from the receiver compared to the transmitter so that the BER is not too high. We choose a to vary from 3×10^{-5} m to 12×10^{-5} m and $b = 12 \times 10^{-5}$ m. As observed in Fig. 12, when a and b become close and the area where the interference source is located becomes further from the receiver, the ratio of $T_{\mathrm{r}}^{\star}$ to T_{b} increases. The BER of the system affected by

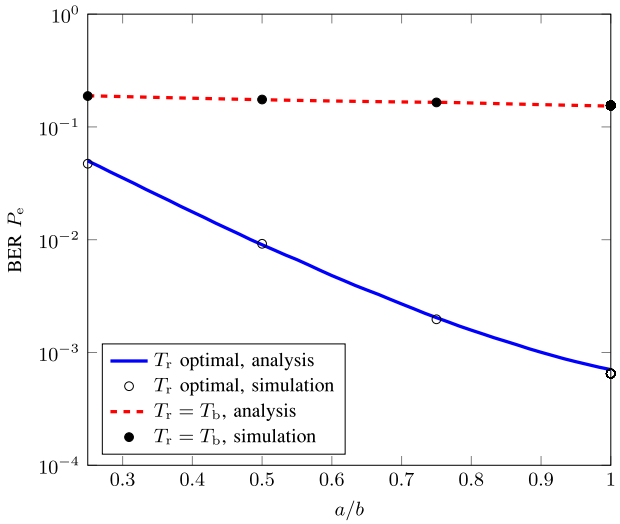

Fig. 13. The BER as a function of a/b when T_{r} is optimized and when $T_{\mathrm{r}} = T_{\mathrm{b}}$ in a 1D system with unknown-location interference.

interference at an unknown location with optimal T_{r} is an improvement on the system with $T_{\mathrm{r}} = T_{\mathrm{b}}$, as shown in Fig. 13. As can be seen, the BER of the system with optimal T_{r} is much lower than the BER of the system with $T_{\mathrm{r}} = T_{\mathrm{b}}$.

VII. Conclusion

In this article, we investigated the optimal detection interval at a receiver in a molecular communication system impaired by external interference. In the 1D and 3D systems affected by external interference, our results showed that the optimal detection interval can be very small compared to the transmission interval. The BER is significantly reduced by optimizing the detection interval compared to when the detection interval is equal to the transmission interval. This also holds true for the system with ISI using the optimal detection interval of the system without ISI. Moreover, we have extended the 1D system model to the case where the exact location of the interference source is unknown to the receiver. The idea of optimizing the detection interval is simple but effective and thus practical for MC systems. Our results can also be extended to MC multi-access networks to improve the network performance and to mobile system where the transceivers and the interference are mobile, which can be considered for future work.

Appendix A
Proof of Lemma 1

When T_{r} changes within the interval $T_{\mathrm{r}}^{(l)} \leq T_{\mathrm{r}} \leq T_{\mathrm{r}}^{(l+1)}$, the values of $P_{Y|X_{\mathrm{T}}}(y|x_{\mathrm{T}} = N_0)$ and $P_{Y|X_{\mathrm{T}}}(y|x_{\mathrm{T}} = N_1)$ also change. However, the relation between $P_{Y|X_{\mathrm{T}}}(y|x_{\mathrm{T}} = N_0)$ and $P_{Y|X_{\mathrm{T}}}(y|x_{\mathrm{T}} = N_1)$, in terms of whether $P_{Y|X_{\mathrm{T}}}(y|x_{\mathrm{T}} = N_0) > P_{Y|X_{\mathrm{T}}}(y|x_{\mathrm{T}} = N_1)$ or $P_{Y|X_{\mathrm{T}}}(y|x_{\mathrm{T}} = N_0) \leq P_{Y|X_{\mathrm{T}}}(y|x_{\mathrm{T}} = N_1)$, is preserved within the interval $T_{\mathrm{r}}^{(l)} \leq T_{\mathrm{r}} \leq T_{\mathrm{r}}^{(l+1)}$. Now, since $\mathbb{Z}_0$ and $\mathbb{Z}_1$ are the sets of discrete Y obtained by comparing $P_{Y|X_{\mathrm{T}}}(y|x_{\mathrm{T}} = N_0)$ and $P_{Y|X_{\mathrm{T}}}(y|x_{\mathrm{T}} = N_1)$, the elements of $\mathbb{Z}_0$ and $\mathbb{Z}_1$ also do not change when T_{r} changes within the interval $T_{\mathrm{r}}^{(l)} \leq T_{\mathrm{r}} \leq T_{\mathrm{r}}^{(l+1)}$. On the other hand, from (5), (6), (7), and (8), we can see that p_d and $p_{d_{\mathrm{I}}}$ are

smooth functions of $T_{\rm r}$. Hence, for $T_{\rm r}^{(l)} \le T_{\rm r} \le T_{\rm r}^{(l+1)}$, $l = 1, 2, \ldots$, and Y belonging to $\mathbb{Z}_0$ or $\mathbb{Z}_1$, $P_{\rm b}$ in (22) is a sum of smooth functions and therefore also a smooth function of $T_{\rm r}$ within this interval. This can be proved strictly by taking the derivative of $P_{\rm b}$ with respect to $T_{\rm r}$ when Y belongs to the fixed sets, $\mathbb{Z}_0$ and $\mathbb{Z}_1$, and when $T_{\rm r}^{(l)} \le T_{\rm r} \le T_{\rm r}^{(l+1)}$ holds. Note that, $P_{\rm b}$ is not smooth at the bounds of these intervals, i.e., $T_{\rm r}^{(l)} \le T_{\rm r} \le T_{\rm r}^{(l+1)}$.

APPENDIX B
DERIVATION OF $P_{\rm b,GAUSSIAN}$ IN (30)

To derive the BER from (14), we need to find $P_{\hat{X}_{\rm T}|X_{\rm T}}(\hat{x}_{\rm T}|x_{\rm T})$. Since $\mathbb{Z}_0$ and $\mathbb{Z}_1$ are now continuous, we rewrite (17) and (18) as follows

$$\begin{aligned}
&P_{\hat{X}_{\rm T}|X_{\rm T}}(\hat{x}_{\rm T} = N_0 | x_{\rm T} = N_1) \\
&\quad = \int_{y\in\mathbb{Z}_0} P_{Y|X_{\rm T}}(y|x_{\rm T} = N_1)\,dy \\
&\quad \overset{(a)}{=} \frac{1}{2}\int_{y\in\mathbb{Z}_0} P_{Y|X_{\rm T},X_{\rm I}}(y|x_{\rm T} = N_1, x_{\rm I} = N_0)\,dy \\
&\qquad + \frac{1}{2}\int_{y\in\mathbb{Z}_0} P_{Y|X_{\rm T},X_{\rm I}}(y|x_{\rm T} = N_1, x_{\rm I} = N_1)\,dy, \quad (36)\\
&P_{\hat{X}_{\rm T}|X_{\rm T}}(\hat{x}_{\rm T} = N_1 | x_{\rm T} = N_0) \quad (37)\\
&\quad = \int_{y\in\mathbb{Z}_1} P_{Y|X_{\rm T}}(y|x_{\rm T} = N_0)\,dy \\
&\quad \overset{(b)}{=} \frac{1}{2}\int_{y\in\mathbb{Z}_1} P_{Y|X_{\rm T},X_{\rm I}}(y|x_{\rm T} = N_0, x_{\rm I} = N_0)\,dy \\
&\qquad + \frac{1}{2}\int_{y\in\mathbb{Z}_1} P_{Y|X_{\rm T},X_{\rm I}}(y|x_{\rm T} = N_0, x_{\rm I} = N_1)\,dy,
\end{aligned}$$

where (a) and (b) follow from (12) and (2), respectively.

Moreover, we have

$$\begin{aligned}
&\int_{\gamma_i}^{\gamma_{i+1}} P_{Y|X_{\rm T},X_{\rm I}}(y|x_{\rm T}, x_{\rm I})\,dy = \\
&\qquad F_{Y|X_{\rm T},X_{\rm I}}(\gamma_{i+1}|x_{\rm T}, x_{\rm I}) - F_{Y|X_{\rm T},X_{\rm I}}(\gamma_i|x_{\rm T}, x_{\rm I}), \quad (38)
\end{aligned}$$

where $F_{Y|X_{\rm T},X_{\rm I}}(\gamma|x_{\rm T}, x_{\rm I})$ is the cumulative distribution function (CDF) of Y given $X_{\rm T}$ and $X_{\rm I}$. $F_{Y|X_{\rm T},X_{\rm I}}(\gamma|x_{\rm T}, x_{\rm I})$ is given by

$$\begin{aligned}
&F_{Y|X_{\rm T},X_{\rm I}}(\gamma|x_{\rm T}, x_{\rm I}) = \frac{1}{2} \\
&\quad \times\left(1 + \operatorname{erf}\left(\frac{\gamma - \left(X_{\rm T}p_d + X_{\rm I}p_{d_{\rm I}}\right)}{X_{\rm T}p_d(1-p_d) + X_{\rm I}p_{d_{\rm I}}(1-p_{d_{\rm I}})}\right)\right). \quad (39)
\end{aligned}$$

Therefore, $\mathbb{Z}_k = \bigcup_i [\gamma_i, \gamma_{i+1}]$ can be written as

$$\begin{aligned}
&\int_{y\in\mathbb{Z}_k} P_{Y|X_{\rm T},X_{\rm I}}(y|x_{\rm T}, x_{\rm I})\,dy \\
&\quad = \sum_i \Big(F_{Y|X_{\rm T},X_{\rm I}}(\gamma_{i+1}|x_{\rm T}, x_{\rm I}) - F_{Y|X_{\rm T},X_{\rm I}}(\gamma_i|x_{\rm T}, x_{\rm I})\Big). \quad (40)
\end{aligned}$$

Inserting (39) into (40), then (40) into (36) and (37), we obtain $P_{\hat{X}_{\rm T}|X_{\rm T}}(\hat{x}_{\rm T}|x_{\rm T})$. Then inserting $P_{\hat{X}_{\rm T}|X_{\rm T}}(\hat{x}_{\rm T}|x_{\rm T})$ and (1) into (14), we obtain the closed-form expression of the BER as in (30).

APPENDIX C
PROOF OF GLOBAL OPTIMUM $T_{\rm r}^{\star}$

To prove that $T_{\rm r}^{\star}$, obtained by Algorithm 1, for the Poisson distribution is globally optimal, we need to prove that when $\mathbb{Z}_0$ and $\mathbb{Z}_1$ are fixed, $P_{\rm b}$ has only one local minimum. This is shown in the following.

Since the sets $\mathbb{Z}_0$ and $\mathbb{Z}_1$ can be obtained by comparing $P_{Y|X_{\rm T}}(y|x_{\rm T} = N_0)$ and $P_{Y|X_{\rm T}}(y|x_{\rm T} = N_1)$ for each y in the interval $0 \le y \le 2N_1$, as shown by (13), $\mathbb{Z}_0$ and $\mathbb{Z}_1$ can be found by solving the following equation

$$P_{Y|X_{\rm T}}(y|x_{\rm T} = N_1) = P_{Y|X_{\rm T}}(y|x_{\rm T} = N_0). \quad (41)$$

If equation (41) has one and only one solution, denoted by $\gamma_{\rm th}$, $\mathbb{Z}_0$ and $\mathbb{Z}_1$ can be written as $\mathbb{Z}_0 = \{0, \ldots, \gamma_{\rm th}\}$ and $\mathbb{Z}_1 = \{\gamma_{\rm th} + 1, \ldots, 2N_1\}$, respectively. Thus, we first prove that (41) has one and only one solution, $\gamma_{\rm th}$. Then, we use $\gamma_{\rm th}$ to derive $P_{\rm b}$ and prove that $\frac{\partial^2 P_{\rm b}}{\partial T_{\rm r}^2} > 0$ with $T_{\rm r}$ satisfying $\frac{\partial P_{\rm b}}{\partial T_{\rm r}} = 0$ when $\mathbb{Z}_0$ and $\mathbb{Z}_1$ are fixed. Moreover, since $P_{\rm b}$ is continuous with respect to $T_{\rm r}$ when $\mathbb{Z}_0$ and $\mathbb{Z}_1$ are fixed, $P_{\rm b}$ has only one local minimal point.

We set the left-hand side and the right-hand side of (41) equal to a constant m, which is then presented by monotonic exponential functions. Thus, the solution of (41) is the solution of the following set of equations

$$\begin{cases}
\left(N_1p_d + N_0p_{d_{\rm I}}\right)^y e^{-\left(N_1p_d + N_0p_{d_{\rm I}}\right)} + \left(N_1p_d + N_1p_{d_{\rm I}}\right)^y \\
\quad \times e^{-\left(N_1p_d + N_1p_{d_{\rm I}}\right)} = m = u\left(N_1p_d + N_1p_{d_{\rm I}}\right)^y \\
\left(N_0p_d + N_0p_{d_{\rm I}}\right)^y e^{-\left(N_0p_d + N_0p_{d_{\rm I}}\right)} + \left(N_0p_d + N_1p_{d_{\rm I}}\right)^y \\
\quad \times e^{-\left(N_0p_d + N_1p_{d_{\rm I}}\right)} = m = v\left(N_0p_d + N_1p_{d_{\rm I}}\right)^y,
\end{cases} \quad (42)$$

where u, v are constants. Since each equation of the set in (42) has only one solution, the solution of the set, i.e., the solution of (41), is unique.

Now, from (27) and the unique $\gamma_{\rm th}$, we have

$$\begin{aligned}
P_{\rm b} = \frac{1}{2} + \frac{1}{4}\Bigg(&\frac{\Gamma(\gamma_{\rm th}+1, N_1p_d + N_0p_{d_{\rm I}})}{\gamma_{\rm th}!} \\
&+ \frac{\Gamma(\gamma_{\rm th}+1, N_1p_d + N_1p_{d_{\rm I}})}{\gamma_{\rm th}!} \\
&- \frac{\Gamma(\gamma_{\rm th}+1, N_0p_d + N_0p_{d_{\rm I}})}{\gamma_{\rm th}!} \\
&- \frac{\Gamma(\gamma_{\rm th}+1, N_0p_d + N_1p_{d_{\rm I}})}{\gamma_{\rm th}!}\Bigg) \quad (43)
\end{aligned}$$

and

$$\begin{aligned}
\frac{\partial P_{\rm b}}{\partial T_{\rm r}} = &\frac{1}{4\gamma_{\rm th}!} \\
&\times\Bigg(-\left(N_1p_d + N_0p_{d_{\rm I}}\right)^{\gamma_{\rm th}} e^{-\left(N_1p_d + N_0p_{d_{\rm I}}\right)}\left(N_1p'_d + N_0p'_{d_{\rm I}}\right) \\
&-\left(N_1p_d + N_1p_{d_{\rm I}}\right)^{\gamma_{\rm th}} e^{-\left(N_1p_d + N_1p_{d_{\rm I}}\right)}\left(N_1p'_d + N_1p'_{d_{\rm I}}\right) \\
&+\left(N_0p_d + N_0p_{d_{\rm I}}\right)^{\gamma_{\rm th}} e^{-\left(N_0p_d + N_0p_{d_{\rm I}}\right)}\left(N_0p'_d + N_0p'_{d_{\rm I}}\right) \\
&+\left(N_0p_d + N_1p_{d_{\rm I}}\right)^{\gamma_{\rm th}} e^{-\left(N_0p_d + N_1p_{d_{\rm I}}\right)}\left(N_0p'_d + N_1p'_{d_{\rm I}}\right)\Bigg). \quad (44)
\end{aligned}$$

When $\frac{\partial P_{\mathrm{b}}}{\partial T_{\mathrm{r}}} = 0$, we have

$$\begin{aligned}
&\left(N_1 p_d + N_0 p_{d_{\mathrm{I}}}\right)^{\gamma_{\mathrm{th}}} e^{-\left(N_1 p_d + N_0 p_{d_{\mathrm{I}}}\right)} \left(N_1 p'_d + N_0 p'_{d_{\mathrm{I}}}\right) = \\
&-\left(N_1 p_d + N_1 p_{d_{\mathrm{I}}}\right)^{\gamma_{\mathrm{th}}} e^{-\left(N_1 p_d + N_1 p_{d_{\mathrm{I}}}\right)} \left(N_1 p'_d + N_1 p'_{d_{\mathrm{I}}}\right) \\
&+\left(N_0 p_d + N_0 p_{d_{\mathrm{I}}}\right)^{\gamma_{\mathrm{th}}} e^{-\left(N_0 p_d + N_0 p_{d_{\mathrm{I}}}\right)} \left(N_0 p'_d + N_0 p'_{d_{\mathrm{I}}}\right) \\
&+\left(N_0 p_d + N_1 p_{d_{\mathrm{I}}}\right)^{\gamma_{\mathrm{th}}} e^{-\left(N_0 p_d + N_1 p_{d_{\mathrm{I}}}\right)} \left(N_0 p'_d + N_1 p'_{d_{\mathrm{I}}}\right).
\end{aligned} \tag{45}$$

From (44), we can derive $\frac{\partial^2 P_{\mathrm{b}}}{\partial T_{\mathrm{r}}^2}$. Then, substituting (45) into $\frac{\partial^2 P_{\mathrm{b}}}{\partial T_{\mathrm{r}}^2}$, we see that

$$\frac{\partial^2 P_{\mathrm{b}}}{\partial T_{\mathrm{r}}^2} > 0. \tag{46}$$

Hence, the stationary point of P_{b} is a minimum. On the other hand, since P_{b} is continuous when $\mathbb{Z}_0$ and $\mathbb{Z}_1$ are fixed, P_{b} has only one minimal point and thus the optimal point given by Algorithm 1 is global optimal.

REFERENCES

[1] T. N. Cao, N. Zlatanov, P. L. Yeoh, and J. Evans, "Optimal detection interval for absorbing receivers in molecular communication systems with interference," in *Proc. IEEE Int. Conf. Commun.*, Kansas City, MO, USA, May 2018, pp. 1–7.

[2] N. Farsad, H. B. Yilmaz, A. Eckford, C. B. Chae, and W. Guo, "A comprehensive survey of recent advancements in molecular communication," *IEEE Commun. Surveys Tuts.*, vol. 18, no. 3, pp. 1887–1919, 3rd Quart., 2016.

[3] T. Nakano, M. J. Moore, F. Wei, A. V. Vasilakos, and J. Shuai, "Molecular communication and networking: Opportunities and challenges," *IEEE Trans. Nanobiosci.*, vol. 11, no. 2, pp. 135–148, Jun. 2012.

[4] C. Xu, S. Hu, and X. Chen, "Artificial cells: From basic science to applications," *Mater. Today*, vol. 19, no. 9, pp. 516–532, 2016.

[5] D. J. Liu and X. Su, "Aptamer biochip for multiplexed detection of biomolecules," U.S. Patent 20 100 240 544 A1, 2010.

[6] M. Turan *et al.*, "Transmitter localization in vessel-like diffusive channels using ring-shaped molecular receivers," *IEEE Commun. Lett.*, vol. 22, no. 12, pp. 2511–2514, Dec. 2018.

[7] V. Jamali, A. Ahmadzadeh, W. Wicke, A. Noel, and R. Schober, "Channel modeling for diffusive molecular communication—A tutorial review," *Proc. IEEE*, vol. 107, no. 7, pp. 1256–1301, Jul. 2019.

[8] A. Noel, K. C. Cheung, and R. Schober, "A unifying model for external noise sources and ISI in diffusive molecular communication," *IEEE J. Sel. Areas Commun.*, vol. 32, no. 12, pp. 2330–2343, Dec. 2014.

[9] C. Jiang, Y. Chen, and K. J. R. Liu, "Inter-user interference in molecular communication networks," in *Proc. IEEE Int. Conf. Acoust. Speech Signal Process.*, Florence, Italy, May 2014, pp. 5725–5729.

[10] I. Llatser, A. Cabellos-Aparicio, M. Pierobon, and E. Alarcón, "Detection techniques for diffusion-based molecular communication," *IEEE J. Sel. Areas Commun.*, vol. 31, no. 12, pp. 726–734, Dec. 2013.

[11] A. Noel, K. C. Cheung, and R. Schober, "Bounds on distance estimation via diffusive molecular communication," in *Proc. IEEE Global Commun. Conf.*, Austin, TX, USA, Dec. 2014, pp. 2813–2819.

[12] A. Noel, K. C. Cheung, and R. Schober, "Optimal receiver design for diffusive molecular communication with flow and additive noise," *IEEE Trans. Nanobiosci.*, vol. 13, no. 3, pp. 350–362, Sep. 2014.

[13] G. D. Ntouni, V. M. Kapinas, and G. K. Karagiannidis, "On the optimal timing of detection in molecular communication systems," in *Proc. Int. Conf. Telecommun.*, Limassol, Cyprus, May 2017, pp. 1–5.

[14] M. Damrath and P. A. Hoeher, "Low-complexity adaptive threshold detection for molecular communication," *IEEE Trans. Nanobiosci.*, vol. 15, no. 3, pp. 200–208, Apr. 2016.

[15] A. C. Heren, H. B. Yilmaz, C. B. Chae, and T. Tugcu, "Effect of degradation in molecular communication: Impairment or enhancement?" *IEEE Trans. Mol. Biol. Multi-Scale Commun.*, vol. 1, no. 2, pp. 217–229, Jun. 2015.

[16] A. Singhal, R. K. Mallik, and B. Lall, "Performance analysis of amplitude modulation schemes for diffusion-based molecular communication," *IEEE Trans. Wireless Commun.*, vol. 14, no. 10, pp. 5681–5691, Oct. 2015.

[17] S. Wang, W. Guo, S. Qiu, and M. D. McDonnell, "Performance of macro-scale molecular communications with sensor cleanse time," in *Proc. Int. Conf. Telecommun.*, Lisbon, Portugal, May 2014, pp. 363–368.

[18] L. S. Meng, P. C. Yeh, K. C. Chen, and I. F. Akyildiz, "MIMO communications based on molecular diffusion," in *Proc. IEEE Global Commun. Conf.*, Anaheim, CA, USA, Dec. 2012, pp. 5602–5607.

[19] B. C. Akdeniz, A. E. Pusane, and T. Tugcu, "Optimal reception delay in diffusion-based molecular communication," *IEEE Commun. Lett.*, vol. 22, no. 1, pp. 57–60, Jan. 2018.

[20] A. Noel, K. Cheung, and R. Schober, "Improving receiver performance of diffusive molecular communication with enzymes," *IEEE Trans. Nanobiosci.*, vol. 13, no. 1, pp. 31–43, Mar. 2014.

[21] N. Farsad, C. Rose, M. Médard, and A. Goldsmith, "Capacity of molecular channels with imperfect particle-intensity modulation and detection," in *Proc. IEEE Int. Symp. Inf. Theory*, Aachen, Germany, Jun. 2017, pp. 2468–2472.

[22] S. K. Tiwari and P. K. Upadhyay, "Maximum likelihood estimation of SNR for diffusion-based molecular communication," *IEEE Wireless Commun. Lett.*, vol. 5, no. 3, pp. 320–323, Jun. 2016.

[23] M. Damrath, S. Korte, and P. A. Hoeher, "Equivalent discrete-time channel modeling for molecular communication with emphasize on an absorbing receiver," *IEEE Trans. Nanobiosci.*, vol. 16, no. 1, pp. 60–68, Jan. 2017.

[24] H. B. Yilmaz and C. B. Chae, "Arrival modelling for molecular communication via diffusion," *Electron. Lett.*, vol. 50, no. 23, pp. 1667–1669, Nov. 2014.

[25] R. Mosayebi, H. Arjmandi, A. Gohari, M. Nasiri-Kenari, and U. Mitra, "Receivers for diffusion-based molecular communication: Exploiting memory and sampling rate," *IEEE J. Sel. Areas Commun.*, vol. 32, no. 12, pp. 2368–2380, Dec. 2014.

[26] N. R. Kim, A. W. Eckford, and C. B. Chae, "Symbol interval optimization for molecular communication with drift," *IEEE Trans. Nanobiosci.* vol. 13, no. 3, pp. 223–229, Sep. 2014.

[27] H. Arjmandi, M. Movahednasab, A. Gohari, M. Mirmohseni, M. Nasiri-Kenari, and F. Fekri, "ISI-avoiding modulation for diffusion-based molecular communication," *IEEE Trans. Mol. Biol. Multi-Scale Commun.*, vol. 3, no. 1, pp. 48–59, Mar. 2017.

[28] A. Marcone, M. Pierobon, and M. Magarini, "Parity-check coding based on genetic circuits for engineered molecular communication between biological cells," *IEEE Trans. Commun.*, vol. 66, no. 12, pp. 6221–6236, Dec. 2018.

[29] M. Mukherjee, H. B. Yilmaz, B. B. Bhowmik, and Y. Lv, "Block synchronization for diffusion-based molecular communication systems," in *Proc. IEEE Int. Conf. Adv. Netw. Telecommun. Syst.*, Indore, India, Dec. 2018, pp. 1–6.

[30] Z. Luo, L. Lin, W. Guo, S. Wang, F. Liu, and H. Yan, "One symbol blind synchronization *in simo* molecular communication systems," *IEEE Wireless Commun. Lett.*, vol. 7, no. 4, pp. 530–533, Aug. 2018.

[31] B. Hsu, P. Chou, C. Lee, and P. Yeh, "Training-based synchronization for quantity-based modulation in inverse gaussian channels," in *Proc. IEEE Int. Conf. Commun.*, Paris, France, May 2017, pp. 1–5.

[32] T. Tung and U. Mitra, "Robust molecular communications: DFE-SPRTs and synchronisation," in *Proc. IEEE Int. Conf. Commun.*, Shanghai, China, May 2019, pp. 1–6.

[33] L. Lin, C. Yang, M. Ma, S. Ma, and H. Yan, "A clock synchronization method for molecular nanomachines in bionanosensor networks," *IEEE Sensors J.*, vol. 16, no. 19, pp. 7194–7203, Oct. 2016.

[34] V. Jamali, A. Ahmadzadeh, and R. Schober, "Symbol synchronization for diffusion-based molecular communications," *IEEE Trans. Nanobiosci.*, vol. 16, no. 8, pp. 873–877, Dec. 2017.

[35] M. Mukherjee, H. B. Yilmaz, B. B. Bhowmik, J. Lloret, and Y. Lv, "Synchronization for diffusion-based molecular communication systems via faster molecules," in *Proc. IEEE Int. Conf. Commun.*, Shanghai, China, May 2019, pp. 1–5.

[36] S. Abadal and I. F. Akyildiz, "Bio-inspired synchronization for nanocommunication networks," in *Proc. IEEE Global Commun. Conf.*, Houston, TX, USA, Dec. 2011, pp. 1–5.

[37] L. Lin, F. Li, M. Ma, and H. Yan, "Synchronization of bio-nanomachines based on molecular diffusion," *IEEE Sensors J.*, vol. 16, no. 19, pp. 7267–7277, Oct. 2016.

[38] M. S. Baptista, F. M. M. Kakmeni, and C. Grebogi, "Combined effect of chemical and electrical synapses in small Hindmarsh–Roseneural networks on synchronisation and the rate of information," *Phys. Rev. E Stat., Nonlinear Soft Matter Phys.*, vol. 82, Sep. 2010, Art. no. 036203.
[39] N. Kopell and B. Ermentrout, "Chemical and electrical synapses perform complementary roles in the synchronization of interneuronal networks," *Proc. Nat. Acad. Sci. USA*, vol. 101, no. 43, pp. 15482–15487, Sep. 2004.
[40] P. G. Ghomsi, F. M. Kakmeni, T. Kofane, and C. Tchawoua, "Synchronization dynamics of chemically coupled cells with activator-inhibitor pathways," *Phys. Lett. A*, vol. 378, no. 38, pp. 2813–2823, Aug. 2014.
[41] I. Nitsan, S. Drori, Y. E. Lewis, S. Cohen, and S. Tzlil, "Mechanical communication in cardiac cell synchronized beating," *Nat. Phys.*, vol. 12, pp. 472–477, Jan. 2016.
[42] M. S. Kuran, H. B. Yilmaz, T. Tugcu, and I. F. Akyildiz, "Modulation techniques for communication via diffusion in nanonetworks," in *Proc. IEEE Int. Conf. Commun. (ICC)*, Jun. 2011, pp. 1–5.
[43] A. Akkaya, H. B. Yilmaz, C. Chae, and T. Tugcu, "Effect of receptor density and size on signal reception in molecular communication via diffusion with an absorbing receiver," *IEEE Commun. Lett.*, vol. 19, no. 2, pp. 155–158, Feb. 2015.
[44] V. Jamali, N. Farsad, R. Schober, and A. Goldsmith, "Non-coherent multiple-symbol detection for diffusive molecular communications," in *Proc. ACM Int. Conf. Nanoscale Comput. Commun.*, vol. 7. New York, NY, USA, Sep. 2016, pp. 1–7.
[45] C. T. Chou, "A Markovian approach to the optimal demodulation of diffusion-based molecular communication networks," *IEEE Trans. Commun.*, vol. 63, no. 10, pp. 3728–3743, Aug. 2015.
[46] H. B. Yilmaz, A. C. Heren, T. Tugcu, and C. Chae, "Three-dimensional channel characteristics for molecular communications with an absorbing receiver," *IEEE Commun. Lett.*, vol. 18, no. 6, pp. 929–932, Jun. 2014.
[47] Y. Lu, M. D. Higgins, A. Noel, M. S. Leeson, and Y. Chen, "The effect of two receivers on broadcast molecular communication systems," *IEEE Trans. Nanobiosci.*, vol. 15, no. 8, pp. 891–900, Dec. 2016.
[48] D. Arifler and D. Arifler, "Monte Carlo analysis of molecule absorption probabilities in diffusion-based nanoscale communication systems with multiple receivers," *IEEE Trans. Nanobiosci.*, vol. 16, no. 3, pp. 157–165, Apr. 2017.
[49] X. Bao, J. Lin, and W. Zhang, "Channel modeling of molecular communication via diffusion with multiple absorbing receivers," *IEEE Wireless Commun. Lett.*, vol. 8, no. 3, pp. 809–812, Jun. 2019.
[50] B. Tepekule, A. E. Pusane, H. B. Yilmaz, C. B. Chae, and T. Tugcu, "ISI mitigation techniques in molecular communication," *IEEE Trans. Mol. Biol. Multi-Scale Commun.*, vol. 1, no. 2, pp. 202–216, Jun. 2015.
[51] T. Cormen, C. Leiserson, R. Rivest, and C. Stein, *Introduction to Algorithms*. Cambridge, MA, USA: MIT Press, 2009.
[52] D. P. Bertsekas, *Convex Optimization Algorithms*. Nashua, NH, USA: Athena Sci., 2015.
[53] J. Nocedal and S. Wright, *Numerical Optimization*. New York, NY, USA: Springer, 2006.
[54] A. Papoulis and S. U. Pillai, *Probability, Random Variables and Stochastic Processes*. New York, NY, USA: McGraw-Hill, 2002.

Trang Ngoc Cao (Member, IEEE) received the B.E. degree in electronics and telecommunications from the Posts and Telecommunications Institute of Technology, Vietnam, in 2012, and the M.S. degree in electronics and radio engineering from Kyung Hee University, South Korea, in 2015. She is currently pursuing the Ph.D. degree with the University of Melbourne, Australia. From 2018 to 2019, she was a Visiting Research Scholar with the Friedrich-Alexander University of Erlangen-Nuremberg, Germany. Her research interests are in communications theory, information theory, and statistical signal processing with a focus on molecular communications. She received several awards, including "Student Travel Grants" for attending the IEEE International Conference on Communications in 2019, the Best Poster Award from the Australian Communication Theory Workshop in 2019, and the Diane Lemaire Scholarship from the Melbourne School of Engineering in 2018.

Nikola Zlatanov (Member, IEEE) was born in North Macedonia. He received the Dipl.Ing. and master's degrees in electrical engineering from Ss. Cyril and Methodius University, Skopje, North Macedonia, in 2007 and 2010, respectively, and the Ph.D. degree from the University of British Columbia (UBC), Vancouver, BC, Canada, in 2015. He is currently a Lecturer (U.S. equivalent to Assistant Professor) with the Department of Electrical and Computer Systems Engineering (ECSE), Monash University, Melbourne, VIC, Australia. His current research interests include wireless communications, information theory, and machine learning. He received several scholarships/awards/grants for his work, including the UBC's Four Year Doctoral Fellowship in 2010, the UBC's Killam Doctoral Scholarship and Macedonia's Young Scientist of the Year in 2011, the Vanier Canada Graduate Scholarship in 2012, the best journal paper award from the German Information Technology Society in 2014, the best conference paper award at ICNC in 2016, and the ARC Discovery Project and ARC DECRA in 2018. He served as an Editor of IEEE COMMUNICATIONS LETTERS from 2015 to 2018.

Phee Lep Yeoh (Member, IEEE) received the B.E. degree (with University Medal) and the Ph.D. degree from the University of Sydney (USYD), Australia, in 2004 and 2012, respectively.

From 2005 to 2008, he was a Wireless Technology Specialist with Telstra, Australia. From 2012 to 2016, he was a Lecturer and Research Fellow of Wireless Communications with the University of Melbourne, Australia. Since 2016, he has been a Senior Lecturer with the School of Electrical and Information Engineering, USYD. His current research interests include secure wireless communications, ultrareliable and low-latency communications, and multiscale molecular communications. He was a recipient of the 2020 USYD Robinson Fellowship, the 2018 Alexander von Humboldt Research Fellowship for Experienced Researchers, and the 2014 Australian Research Council Discovery Early Career Researcher Award. He has received the best paper awards at IEEE ICC 2014 and IEEE VTC-Spring 2013, and the best student paper awards with his supervised students at the 2013, and the 2019 Australian Communications Theory Workshop.

Jamie S. Evans (Senior Member, IEEE) was born in Newcastle, NSW, Australia, in 1970. He received the B.S. degree in physics and the B.E. degree in computer engineering from the University of Newcastle, in 1992 and 1993, respectively, where he received the University Medal upon graduation, and the M.S. and Ph.D. degrees in electrical engineering from the University of Melbourne, Australia, in 1996 and 1998, respectively, and was awarded the Chancellor's Prize for excellence for his Ph.D. thesis. From March 1998 to June 1999, he was a Visiting Researcher with the Department of Electrical Engineering and Computer Science, University of California, Berkeley. Since returning to Australia in July 1999, he has been held academic positions with the University of Sydney, the University of Melbourne, and Monash University. He is currently a Professor and the Deputy Dean of the Melbourne School of Engineering, University of Melbourne. His research interests are in communications theory, information theory, and statistical signal processing with a focus on wireless communications networks.